Am J Cancer Res 2022;12(12):5462-5483
www.ajcr.us /ISSN:2156-6976/ajcr0146420

Original Article

Sumoylation participates in the regulation of YB-1-mediated mismatch repair deficiency and alkylator tolerance

Ru-Tsun Mai[1,3], Chi-Hong Chao[1,2,3], Yao-Wen Chang[4], Yu-Ching Kao[1,3], Yi Cheng[2,3], Hsiang-Yu Hsu[2,3], Yi-Yuan Su[1,3], Chen-Yun Wang[2,3], Bo-Ying Lai[4]

[1]Department of Biological Science and Technology, College of Biological Science and Technology, National Yang Ming Chiao Tung University, Hsinchu 300, Taiwan; [2]Institute of Molecular Medicine and Bioengineering, College of Biological Science and Technology, National Yang Ming Chiao Tung University, Hsinchu 300, Taiwan; [3]Center for Intelligent Drug Systems and Smart Bio-devices (IDS[2]B), National Yang Ming Chiao Tung University, Hsinchu 300, Taiwan; [4]Institute of Biochemistry and Molecular Biology, School of Life Sciences, National Yang Ming Chiao Tung University, Taipei 112, Taiwan

Received September 10, 2022; Accepted November 27, 2022; Epub December 15, 2022; Published December 30, 2022

Abstract: Numerous reports indicate that enhanced expression of Y-box binding protein-1 (YB-1) in tumor cells is strongly associated with tumorigenesis, aggressiveness, drug resistance, as well as poor prognosis in several types of cancers, and YB-1 is considered to be an oncogene. The molecular mechanism contributing to the regulation of the biological activities of YB-1 remains obscure. Sumoylation, a post-translational modification involving the covalent conjugation of small ubiquitin-like modifier (SUMO) proteins to a target protein, plays key roles in the modulation of protein functions. In this study, our results revealed that YB-1 is sumoylated and that Lys^{26} is a critical residue for YB-1 sumoylation. Moreover, YB-1 was found to directly interact with SUMO proteins, and disruption of the SUMO-interacting motif (SIM) of YB-1 not only interfered with this interaction but also diminished YB-1 sumoylation. The subcellular localization, protein stability, and transcriptional regulatory activity of YB-1 were not significantly affected by sumoylation. However, decreased sumoylation disrupted the interaction between YB-1 and PCNA as well as YB-1-mediated inhibition of the MutSα/PCNA interaction and MutSα mismatch binding activity, indicating a functional role of YB-1 sumoylation in inducing DNA mismatch repair (MMR) deficiency and spontaneous mutations. The MMR machinery also recognizes alkylator-modified DNA adducts to signal for cell death. We further demonstrated that YB-1 sumoylation is crucial for the inhibition of S_N1-type alkylator MNNG-induced cytotoxicity, G2/M-phase arrest, apoptosis, and the MMR-dependent DNA damage response. Collectively, these results provide molecular explanations for the impact of YB-1 sumoylation on MMR deficiency and alkylator tolerance, which may provide insight for designing therapeutic strategies for malignancies and alkylator-resistant cancers associated with YB-1 overexpression.

Keywords: YB-1, sumoylation, SUMO-interacting motif, DNA mismatch repair, DNA damage response, alkylator tolerance

Introduction

Y-box binding protein-1 (YB-1) interacts with DNA/RNA and numerous other cellular partners, and is thereby involved in the regulation of a wide spectrum of cellular processes [1-4]. Evidences provided by extensive studies strongly indicate that enhanced expression or nuclear accumulation of YB-1 closely correlates with tumorigenesis, tumor growth, epithelial-mesenchymal transition (EMT), invasion, metastasis, angiogenesis, chemotherapeutic resistance, and cancer stemness, which contribute to all of "the Hallmarks of Cancer" and to poor prognosis in patients with diverse cancer [1, 5-11]. Thus, YB-1 functions as an oncogene and is considered a potential biomarker for and therapeutic target for various types of cancers [5-7, 11, 12].

Various post-translational modifications (PTMs) occur on YB-1, including ubiquitination, phos-

phorylation, acetylation, methylation, poly(ADP-ribosyl)ation, and *O*-GlcNAcylation, which modulate its biological properties and participate in the regulation of different cellular processes [3, 11-15]. Among these modifications, phosphorylation of YB-1 at Ser^{102}, which induces its nuclear translocation, regulates the transcription of growth-related genes, causes EMT, activates the translation of stress- and growth-related mRNAs, and promotes drug resistance as well as cancer stemness, is currently the most extensively studied [2, 3, 10, 12, 13]. Notably, a previous study indicated that zebrafish YB-1 (zfYB-1) participates in circadian control and implicates sumoylation of zfYB-1 in the regulation of this function [16]. However, whether human YB-1 is modified through the sumoylation pathway remains unclear.

Sumoylation affects the biological properties of target proteins and plays important roles in diverse biological processes and diseases [17-21]. Sumoylation involves the covalent conjugation of small ubiquitin-like modifier (SUMO) proteins to specific lysine residues of a target protein through an enzymatic cascade comprising the SUMO-activating enzyme SAE1/SAE2 (E1), the SUMO-conjugating enzyme Ubc9 (E2), and a SUMO E3 ligase [19, 20, 22, 23]. In human cells, three SUMO paralogs, SUMO-1, SUMO-2, and SUMO-3, are responsible for sumoylation [21, 22, 24]. SUMO-2 and SUMO-3 share 97% amino acid sequence identity [19, 21, 22], and each contains a sumoylation site in its N-terminal region for the formation of a poly-SUMO chain [21, 25]. Sumoylation sometimes occurs at a lysine residue within a consensus Ubc9-binding motif ΨKxD/E (Ψ: an aliphatic branched amino acid; x: any residue) [19, 22]; however, the majority of sumoylated proteins do not possess such a motif [26, 27]. In addition, the SUMO-interacting motif (SIM), with a short hydrophobic core, mediates non-covalent binding of SIM-containing proteins to SUMO proteins or sumoylated factors [19, 22, 28, 29]. Many SUMO targets, such as Daxx and ubiquitin-specific protease 25 (USP25), also contain a SIM, which is essential for sumoylation of these proteins [30, 31].

DNA mismatch repair (MMR) protects genome integrity by correcting base mismatches and insertion/deletion loops (IDLs) during DNA replication and other biological processes [32-35]. MMR deficiency often leads to the accumulation of spontaneous mutations and correlates with several types of cancers [32, 36-40]. In eukaryotic cells, MMR is initiated when MutSα (the MSH2/MSH6 heterodimer) recognizes single-base mismatches or IDLs with 1-2 extrahelical nucleotides, whereas MutSβ (the MSH2/MSH3 heterodimer) recognizes larger IDLs [41-43]. Then, MMR-related factors are recruited sequentially to eliminate error-containing DNA and resynthesize error-free DNA [41, 42, 44-46]. In this process, proliferating cell nuclear antigen (PCNA) interacts with several PCNA-interacting protein (PIP)-box-containing MMR proteins, such as MutSα and MutSβ, which greatly enhances MMR activity [34, 43, 44, 47]. Our previous study indicated that YB-1 interacts with PCNA and inhibits the MutSα/PCNA interaction, thereby preventing MutSα from recognizing mismatches and resulting in MMR deficiency [48]. Thus, YB-1 serves as a negative regulator of MMR and predisposes cells to genomic instability with an increased frequency of spontaneous mutation.

MMR is also responsible for recognizing alkylator-modified DNA and sensitizes cells to treatment with alkylators, such as the S_N1-type mono-functional alkylators Temozolomide and *N*-methyl-*N'*-nitro-*N*-nitrosoguanidine (MNNG) [32, 49-51]. Among the several methylated base adducts, O^6-methylguanine (O^6-meG) is the most mutagenic and cytotoxic lesion [49, 52] and is repaired by O^6-meG-DNA methyltransferase (MGMT). However, transferring the methyl group of O^6-meG to the active site of MGMT results in the inactivation of this enzyme [52]. Unrepaired O^6-meG can pair with thymine (T) bases during DNA replication to form O^6-meG:T mismatches, which are recognized by MutSα to initiate MMR and activate the DNA damage response [32, 49-51, 53]. The "futile repair cycle" and "direct signaling" models have been proposed to explain the molecular mechanism of the MMR-dependent DNA damage response. Upon alkylator insult, several components of DNA damage response signaling, such as ataxia telangiectasia mutated (ATM), ATM- and Rad3-related (ATR), checkpoint kinase 1 (Chk1), and Chk2, are activated, which ultimately induces cell cycle arrest and cell death [32, 49-51]. Hence, MMR-deficient tumors exhibit alkylator tolerance with increased cell

viability after alkylator-based chemotherapy [49, 51, 54].

In this study, we found that YB-1 is modified by the sumoylation pathway, possibly through its direct interaction with SUMO proteins. The important SUMO acceptor lysine residues and a putative SIM in YB-1 were identified, and the integrity of the SIM was found to be crucial for YB-1 sumoylation. Interestingly, our results indicated that the sumoylation level of YB-1 is positively correlated with its PCNA binding affinity, suggesting a regulatory role of YB-1 sumoylation in YB-1-mediated MMR deficiency. Our observations supported this hypothesis. Sumoylation of YB-1 is important for its inhibition of the MutSα/PCNA interaction and the mismatch binding activity of MutSα, which plays a functional role in increasing the spontaneous mutation frequency. In addition, YB-1 and its sumoylation reduce cell susceptibility to MNNG treatment, which induces early escape from G2/M-phase arrest, inhibits apoptosis, and suppresses the MMR-dependent DNA damage response. These findings may provide mechanistic explanations for YB-1-induced tumorigenesis and alkylator tolerance.

Materials and methods

Plasmids

The plasmids pcDNA3/HA-YB-1, pGST-YB-1, and pCMV2/FLAG-YB-1 have been described previously [48, 55]. Lysine-to-arginine (K/R) or valine-to-alanine (V/A) substitution of specific amino acid residues in the YB-1 coding sequence in pcDNA3/HA-YB-1, pGST-YB-1, or pCMV2/FLAG-YB-1 was carried out by using a QuikChange Lightning Site-Directed Mutagenesis Kit (Stratagene, La Jolla, CA, USA) with proper plasmid templates and primers according to the manufacturer's instructions. The sequences of the primers used for oligonucleotide-directed mutagenesis are listed in Table S1. The pcDNA3/His-SUMO-1 plasmid was kindly provided by Dr. Tzu-Hao Cheng (Institute of Biochemistry and Molecular Biology, National Yang Ming Chiao Tung University, Taipei, Taiwan). The pcDNA3/His-SUMO-2 and pcDNA3/His-SUMO-3 plasmids were constructed by replacing the SUMO-1 complementary DNA (cDNA) fragment in pcDNA3/His-SUMO-1 with the *Bam*HI/*Xho*I-digested full-length SUMO-2 or SUMO-3 cDNA fragment, respectively. The pcDNA-SRα/FLAG-Ubc9 plasmid was generated by insertion of the full-length Ubc9 cDNA fragment into the *Eco*RI/*Apa*I-digested pcDNA-SRα/FLAG vector [56]. The GST-YB-1 deletion constructs pGST-YB-1/1-60, pGST-YB-1/61-125, pGST-YB-1/61-130, pGST-YB-1/126-324, pGST-YB-1/130-230, and pGST-YB-1/231-324 were generated by insertion of a PCR-amplified *Bam*HI/*Xho*I-digested fragment of the indicated YB-1 coding region into the *Bam*HI/*Xho*I-digested pGEX-5X-1 vector (GE Healthcare, Chicago, IL, USA). To generate the bacterial His-tagged SUMO paralog expression constructs, the plasmids pET28a/His-SUMO-1 and pET-28a/His-SUMO-3 were constructed by inserting a cDNA fragment of full-length SUMO-1 and SUMO-3, respectively, into the *Bam*HI/*Xho*I-digested pET28a vector (Novagen, Madison, WI, USA). The reporter plasmid pMDRP1.5-Luc was constructed by insertion of a *Xho*I/*Hind*III-digested fragment of the human *multidrug resistance-1* (*MDR-1*) upstream promoter (nucleotide positions -1500 to +1 relative to the transcription initiation site) into the *Xho*I/*Hind*III-digested pGL2-Basic vector (Promega, Madison, WI, USA). The promoter region of *MDR-1* was PCR amplified from pMDRP1.7-CAT [57].

Antibodies

The following antibodies were used in this study: anti-hemagglutinin (HA) tag (MMS-101R, Covance, Emeryville, CA, USA), anti-HA-peroxidase (#12013819001, Roche Applied Science, Indianapolis, IN, USA), anti-FLAG tag (ab1257, Abcam, Cambridge, UK), anti-His tag (#70796-4, Novagen, Madison, WI, USA), anti-YB-1 (ab76149, Abcam), anti-SUMO-1 (ab32058, Abcam), anti-SUMO-3 (ab34661, Abcam), anti-PCNA (sc-56, Santa Cruz Biotechnology, Dallas, TX, USA), anti-MSH6 (#610919, BD Biosciences, Lexington, KY, USA), anti-MSH2 (Ab-2, Calbiochem, Darmstadt, Germany), anti-ATR (A300-138A, Bethyl Laboratories, Montgomery, TX, USA), anti-ATM (A300-299A, Bethyl Laboratories), anti-Chk1 (sc-8408, Santa Cruz Biotechnology), anti-Chk2 (#6334, Cell Signaling Technology, Danvers, MA, USA), anti-H2A.X (#2595, Cell Signaling Technology), anti-phospho-ATR (Ser^{428}, #2853, Cell Signaling Technology), anti-phospho-ATM (Ser^{1981}, #5883, Cell Signaling Technology), anti-phospho-Chk1 (Ser^{345}, #2348, Cell Signaling Technology), anti-phospho-Chk2 (Thr^{68}, #2197, Cell Signaling Techno-

logy), anti-phospho-H2A.X (Ser^{139}, #9718, Cell Signaling Technology), anti-MGMT (sc-166491, Santa Cruz Biotechnology), and anti-β-actin (AC-15, Sigma-Aldrich, St. Louis, MO, USA). The production of anti-GST-YB-1 antibodies has been described previously [48]. Purified full-length His-SUMO-1 and His-SUMO-3 were also used for the generation of rabbit polyclonal anti-SUMO-1 and anti-SUMO-3 antibodies, respectively (LTK BioLaboratories, New Taipei City, Taiwan).

Cell culture, plasmid transfection, and establishment of permanent cell lines

Human embryonic kidney HEK293T and human cervical adenocarcinoma HeLa cells were cultured in Dulbecco's modified Eagle's medium (DMEM) supplemented with 10% inactivated fetal bovine serum (#10437-028, Gibco, Grand Island, NY, USA), 1% non-essential amino acids, 100 units/ml penicillin, and 100 μg/ml streptomycin. Cells were incubated in a humidified incubator (Forma 301, Thermo Fisher Scientific, Marietta, OH, USA) at 37°C with 5% CO_2. Plasmids were transfected into HEK293T or HeLa cells by the calcium phosphate coprecipitation method as previously described [58]. Cells were washed twice with phosphate-buffered saline (PBS) 16-20 h after transfection. HeLa cells were also transfected with Lipofectamine 2000 transfection reagent according to the manufacturer's instructions (Invitrogen, Karlsruhe, Germany), and the cells were washed once with PBS 6 h after transfection. To establish the cells lines with stable wild-type or mutant YB-1 overexpression and the corresponding vector control cell lines, plasmids expressing wild-type or mutant HA-YB-1 and the HA vector were transfected into HeLa cells with Lipofectamine 2000 transfection reagent. Twenty-four hours post transfection, cells (10^5 cells/10-cm dish) were reseeded and selected using 450 μg/ml G418 (#11811, Gibco) for 14 days. Single colonies of G418-resistant cells were picked and amplified, and the expression levels of wild-type and mutant YB-1 were examined by western blotting.

In vivo sumoylation assay

The *in vivo* sumoylation assay was performed as previously described [59]. Forty-eight hours post transfection, HEK293T cells were harvested with PBS in the presence of 10 mM N-ethylmaleimide (Sigma-Aldrich) and separated into two aliquots. One aliquot was used to analyze the expression of transfected proteins by western blotting with the appropriate antibodies. The other aliquot of the cell pellet was resuspended in buffer A (6 M guanidinium-HCl, 0.1 M Na_2HPO_4/NaH_2PO_4, 0.01 M Tris-Cl [pH 8.0], 10 mM N-ethylmaleimide, 5 mM imidazole, 0.1% NP-40, and 0.1% 2-mercaptoethanol), and cell lysates (500-800 μg) were incubated with 20 μl of Ni-NTA beads (Novagen) for 4 h at room temperature. The beads were then washed twice with buffer A, buffer B (8 M urea, 0.1 M Na_2HPO_4/NaH_2PO_4, 0.01 M Tris-Cl [pH 8.0], 0.1% NP-40, and 0.1% 2-mercaptoethanol), and buffer C (8 M urea, 0.1 M Na_2HPO_4/NaH_2PO_4, 0.01 M Tris-Cl [pH 6.3], 0.1% NP-40, and 0.1% 2-mercaptoethanol). The proteins bound to the beads were eluted with buffer D (200 mM imidazole, 0.15 M Tris-Cl [pH 6.7], 0.2 M dithiothreitol, 5% sodium dodecyl sulfate, and 30% glycerol) and analyzed by western blotting with anti-HA-peroxidase antibodies.

Purification of recombinant protein, in vitro sumoylation assay, and in vitro binding assay

The steps for purification of recombinant wild-type and mutant GST-YB-1 fusion proteins as well as His-tagged SUMO-1 and SUMO-3 in *E. coli* BL21 (DE3) were described previously [58]. The *in vitro* sumoylation assay was conducted with the GST-YB-1 variants by using the SUMOlink SUMO-1 Kit (#40120, Active Motif, Carlsbad, CA, USA) and SUMOlink SUMO-2/3 Kit (#40220, Active Motif) according to the manufacturer's instructions. For the *in vitro* binding assay, 20 μl of glutathione-Sepharose 4B beads (GE Healthcare) containing GST or the GST-YB-1 variants was incubated with His-tagged SUMO-1 or SUMO-3 protein in PBS containing 0.5% NP-40 and 100 mM imidazole at 4°C for 3 h. The beads were washed and treated with sodium dodecyl sulfate-polyacrylamide gel electrophoresis (SDS-PAGE) sample buffer, and the eluted proteins were analyzed by western blotting with an anti-SUMO-1 or anti-SUMO-3 antibody. Alternatively, an *in vitro* binding assay was carried out by incubating purified GST-YB-1 variants and His-SUMO-3 in PBS containing 0.5% NP-40 and 100 mM imidazole at 4°C for 3 h. Then, 20 μl of Ni-NTA beads (Novagen) was added and incubated at 4°C for 30 min. The beads were washed and treated with SDS-PAGE sample buffer, and the eluted

proteins were analyzed by western blotting with anti-GST-YB-1 antibodies.

Immunofluorescence staining and confocal microscopy

HeLa cells were transfected with plasmids expressing HA-YB-1 variants by Lipofectamine 2000 transfection reagent. Forty-eight hours post transfection, the cells were reseeded on coverslips and incubated overnight. Cells were fixed with precooled (-20°C) methanol:acetone (1:1), incubated with 5% BSA/PBS at 4°C for 1 h, and subsequently incubated first with an anti-HA tag primary antibody at 4°C overnight and then with Alexa Fluor 488-conjugated goat anti-mouse IgG as the secondary antibody (A-11001, Invitrogen) at room temperature for 1 h. The primary and secondary antibodies were diluted in PBS containing 1% BSA. Then, nuclei were stained with 4',6-diamidino-2-phenylindole (DAPI), and the coverslips were mounted with Dako fluorescence mounting medium (S3023, Agilent Technologies, Santa Clara, CA, USA). Images were acquired with a multiphoton confocal microscope system (TCS-SP5-X AOBS, Leica, Germany).

Protein half-life assay and reporter activity assay

A protein half-life assay similar to that previously described was performed [55]. Briefly, HeLa cells were transfected with plasmids expressing the HA-YB-1 variants by the calcium phosphate coprecipitation method. Forty-eight hours post transfection, the cells were treated with 100 μg/ml cycloheximide (Sigma-Aldrich) and then harvested at the indicated time points. The protein levels of the HA-YB-1 variants were analyzed by western blotting with an anti-HA tag antibody. For analysis of luciferase activity, HeLa cells (2×10^5 cells/well of a 6-well plate) were transfected with pMDRP1.5-Luc alone or together with different amounts of plasmid expressing HA-YB-1 or HA-YB-1/K26R by the calcium phosphate coprecipitation method. Forty-eight hours post transfection, a luciferase assay was carried out as previously described [60].

Subcellular fractionation and biotinylated DNA pull-down assay

Nuclear extracts were prepared according to the method described previously [60]. A biotinylated DNA pull-down assay was performed as described previously [48], except that nuclear extracts of cells with stable overexpression of wild-type or mutant HA-YB-1 and the corresponding vector control cells were used.

Co-immunoprecipitation

To examine the interactions between PCNA and YB-1 variants, HEK293T cells were transfected with the FLAG vector or plasmids expressing the FLAG-YB-1 variants. Forty-eight hours post transfection, the cells were resuspended in lysis buffer (0.5% NP-40, 10 mM N-ethylmaleimide, and 1 × protease inhibitor cocktail in PBS), and cell extracts (500 μg) were immunoprecipitated with 20 μl of anti-FLAG M2 magnetic beads (Sigma-Aldrich) at 4°C overnight. The beads were washed three times with lysis buffer and treated with SDS-PAGE sample buffer. Proteins bound to the beads were analyzed by western blotting with anti-FLAG tag and anti-PCNA antibodies. To investigate complex formation among PCNA, MutSα, and YB-1 variants, nuclear extracts (250 μg) of cells with stable overexpression of wild-type or mutant HA-YB-1 and the corresponding vector control cells were incubated with 2 μg of an anti-PCNA antibody in co-immunoprecipitation buffer (5 mM HEPES-KOH (pH 7.9), 80 mM NaCl, 0.25% NP-40, 0.25 mM $MgCl_2$, 0.1 mM EDTA, 0.1 mM EGTA, 10 mM N-ethylmaleimide, and 1 × protease inhibitor cocktail) at 4°C overnight. Then 20 μl of Protein G-Sepharose beads (GE Healthcare) was added and incubated at 4°C for 3 h. After washing three times with co-immunoprecipitation buffer, the bound fractions were eluted in SDS-PAGE sample buffer and subjected to western blotting with anti-MSH6, anti-MSH2, anti-HA tag, and anti-PCNA antibodies.

Ouabain resistance assay and colony formation assay

To evaluate the spontaneous mutation frequency, mutations in the *Na^+/K^+ ATPase α1 subunit* resulting in ouabain-resistant cells were analyzed by an ouabain resistance assay as previously described [48], except that cells with stable overexpression of wild-type or mutant HA-YB-1 and the corresponding vector control cells were used. For the colony formation assay, cells were incubated overnight in complete medium with or without 25 μM O^6-benzylguanine. Before 3 h of MNNG treat-

ment, another dose of O^6-benzylguanine was added to the O^6-benzylguanine-treated cells. Then, the cells were treated with 0.05 μM MNNG for 3 h. The cells treated with MNNG only were reseeded at a density of ~300 cells per 10-cm dish in complete medium, while the O^6-benzylguanine/MNNG-treated cells were reseeded at ~1200 cells per 10-cm dish in complete medium containing 25 μM O^6-benzylguanine. During the subsequent 14 days of incubation, the culture medium was replaced every 2 or 3 days, and medium containing 25 μM O^6-benzylguanine was used for O^6-benzylguanine/MNNG-treated cells. Colonies were fixed with 1:1 acetone:methanol and stained with 0.05% crystal violet.

Flow cytometric analyses of DNA content and apoptosis

For analysis of MNNG-induced G2/M-phase arrest, cells with stable overexpression of wild-type or mutant HA-YB-1 and the corresponding vector control cells were treated with 25 μM O^6-benzylguanine and 0.05 μM MNNG as described above. At the indicated time points after MNNG treatment, cells were collected by trypsinization, resuspended in PBS, fixed with absolute ethanol by dropwise application to a final concentration of ~70%, and incubated at -20°C overnight. Cells were stained with PBS containing 50 μg/ml propidium iodide, 0.1% Triton X-100, and 200 μg/ml DNase-free RNase A at room temperature for 30 min. Stained cells were analyzed by using a FACSCalibur flow cytometer (BD Biosciences). Analysis of the cell population in each cell cycle phase was performed by ModFit LT 5.0 software (Verity Software House, Topsham, ME, USA). For analysis of MNNG-induced apoptosis, cells were treated with 25 μM O^6-benzylguanine and 0.05 μM MNNG as described above and collected at 96 h post MNNG treatment. Cells were stained by using an Annexin V-FITC Apoptosis Detection Kit (Strong Biotech, Taipei, Taiwan) according to the manufacturer's instructions. Analysis of apoptotic cells was carried out by using a FACSCalibur flow cytometer (BD Biosciences).

Results

YB-1 is sumoylated by three SUMO paralogs

An *in vivo* sumoylation assay, as previously described [59], was established in our laboratory. In this method, His-tagged SUMOs and HA-tagged target protein were exogenously expressed in cells. Then, the cells were lysed under denaturing conditions in the presence of the isopeptidase inhibitor N-ethylmaleimide, and sumoylated proteins were captured on Ni-NTA beads and analyzed by immunoblotting with an anti-HA tag antibody. To assess whether YB-1 can be modified by SUMO proteins, plasmids expressing HA-YB-1, His-SUMO-3, and FLAG-Ubc9 were co-transfected in different combinations into HEK-293T cells, and the cell lysates were then used for the *in vivo* sumoylation assay. An HA-tagged protein species that exhibited an increased molecular weight of ~20 kDa, similar to that of SUMO-modified HA-YB-1, was observed (**Figure 1A**, lane 3), implying that SUMO-3 can be conjugated to YB-1. The amount of this HA-tagged protein species was increased by overexpression of the E2 SUMO-conjugating enzyme Ubc9 (**Figure 1A**, compare lane 4 to lane 3) and was also detected by an anti-YB-1 antibody when the same western blot membrane was reprobed with this antibody. These findings indicate that YB-1 is a target of the sumoylation pathway.

Next, we investigated whether other SUMO paralogs can be conjugated to YB-1. To this end, a similar *in vivo* sumoylation assay was carried out, and plasmids expressing His-SUMO-1 and His-SUMO-2 were also used in this experiment. As shown in **Figure 1B**, higher-molecular-weight HA-YB-1 species were detected when cells were co-transfected with plasmids expressing HA-YB-1 and His-SUMOs (lanes 3, 5, and 7), and the abundances of these species were increased by overexpression of Ubc9 (compare lanes 4, 6, and 8 to lanes 3, 5, and 7, respectively). These results revealed that SUMO-1, SUMO-2, or SUMO-3 can be conjugated to YB-1.

Lys^{26} plays an important role in YB-1 sumoylation

To address the possible roles of YB-1 sumoylation in cellular processes, we identified SUMO acceptor lysine residue(s) in YB-1. YB-1 does not contain the typical ΨKxD/E motif for SUMO conjugation, but it possesses two non-canonical ($TK^{81}ED$ and $EK^{170}NE$) sumoylation sites and one inverted ($ETK^{304}A$) sumoylation site (**Figure 2A**), as predicted by GPS-SUMO 1.0 software

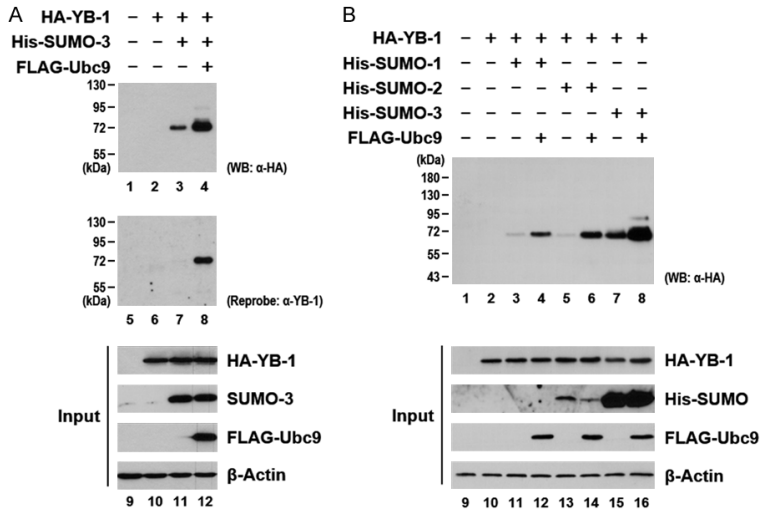

Figure 1. YB-1 can be sumoylated *in vivo*. (A) Plasmids expressing HA-YB-1, His-SUMO-3, and FLAG-Ubc9 were co-transfected into HEK293T cells as indicated. To isolate His-SUMO-conjugated proteins, cells were harvested 48 h post transfection and subjected to an *in vivo* sumoylation assay in the presence of N-ethylmaleimide. Proteins bound to the beads were analyzed by western blotting with an anti-HA-peroxidase antibody (lanes 1-4), and the same blot was then stripped and reprobed with an anti-YB-1 antibody (lanes 5-8). To confirm the expression of transfected proteins, whole-cell lysates were analyzed by immunoblotting using antibodies against the HA tag, SUMO-3, the FLAG tag, and β-actin. (B) An *in vivo* sumoylation assay similar to that described in (A) was performed, except that plasmids expressing His-SUMO-1 and His-SUMO-2 were also used (lanes 1-8). Whole-cell lysates were subjected to western blotting using antibodies against the HA tag, the His tag, the FLAG tag, and β-actin (lanes 9-16). β-Actin was used as a loading control.

(http://sumosp.biocuckoo.org/). By using an *in vivo* sumoylation assay with plasmids expressing HA-YB-1/K81R, HA-YB-1/K170R, HA-YB-1/K301.304R, and HA-YB-1/K81.170R, we found that the sumoylation status of these YB-1 mutants was not altered when these lysine (K) residues were substituted with arginine (R) (Figure S1A, lanes 7, 14, 17, and 18). However, the sumoylation level of YB-1/K26R was significantly reduced in cells overexpressing either His-SUMO-1 (**Figure 2B**, lane 3 and Figure S1A, lane 3) or His-SUMO-3 (**Figure 2C**, lane 3), indicating that Lys^{26} is important for the sumoylation of YB-1. As YB-1 sumoylation was not completely disrupted by the K26R mutation, there might be additional sumoylation sites in YB-1. To further clarify the roles of sumoylation in the biological functions of YB-1, the SUMO acceptor lysine residue(s) other than Lys^{26} in YB-1 were explored. Thus, multiple K/R mutants of HA-YB-1, in addition to the K26R mutation, were expressed, and the sumoylation status of these multiple K/R HA-YB-1 variants was evaluated by using an *in vivo* sumoylation assay. Among these mutants, YB-1/K26.301.304R exhibited the lowest sumoylation level (Figure S1B, lane 18; **Figure 2B**, lane 7; **Figure 2C**, lane 7). Notably, the sumoylation status of both YB-1/K26.301R and YB-1/K26.304R was similar to that of YB-1/K26R (compare lanes 5 and 6 with lane 3 in **Figure 2B** and **2C**), and YB-1/K301.304R was modified by SUMOs to levels similar to those of wild-type YB-1 (compare lane 4 with lane 2 in **Figure 2B** and **2C**). These observations suggested that Lys^{26} is important for YB-1 sumoylation and that simultaneous mutations in Lys^{26}, Lys^{301}, and Lys^{304} of YB-1 have the most significant effect on its sumoylation.

The sumoylation status of YB-1 was further confirmed by using an *in vitro* sumoylation assay with purified GST-YB-1 and its variants (**Figure 2D**). As shown in **Figure 2E**, GST-YB-1 was sumoylated by the three SUMO paralogs *in vitro*, and two major higher-molecular-weight species representing sumoylated GST-YB-1 were observed (lanes 2-4). In the sumoylation reactions with GST-YB-1/K26R and SUMO-2 or SUMO-3, the abundance of the upper higher-molecular-weight species was reduced (lanes 7-8) compared to that of GST-YB-1 (lanes 3-4), while this upper species was not detected in the reaction with GST-YB-1/K26R and SUMO-1 (lane 6). As SUMO-1 does not contain a ΨKxD/E motif and is unable to form poly-SUMO chain like SUMO-2/3 can [61], this finding indicated that there are additional SUMO acceptor lysine residues other than Lys^{26} in YB-1. In line with this observation, the higher-molecular-weight species were absent in the reaction with GST-YB-1/K26.301.304R (**Figure 2F**, lanes 5-7), strengthening the conclusion that simultaneous mutations in Lys^{26}, Lys^{301}, and Lys^{304} greatly affect YB-1 sumoylation.

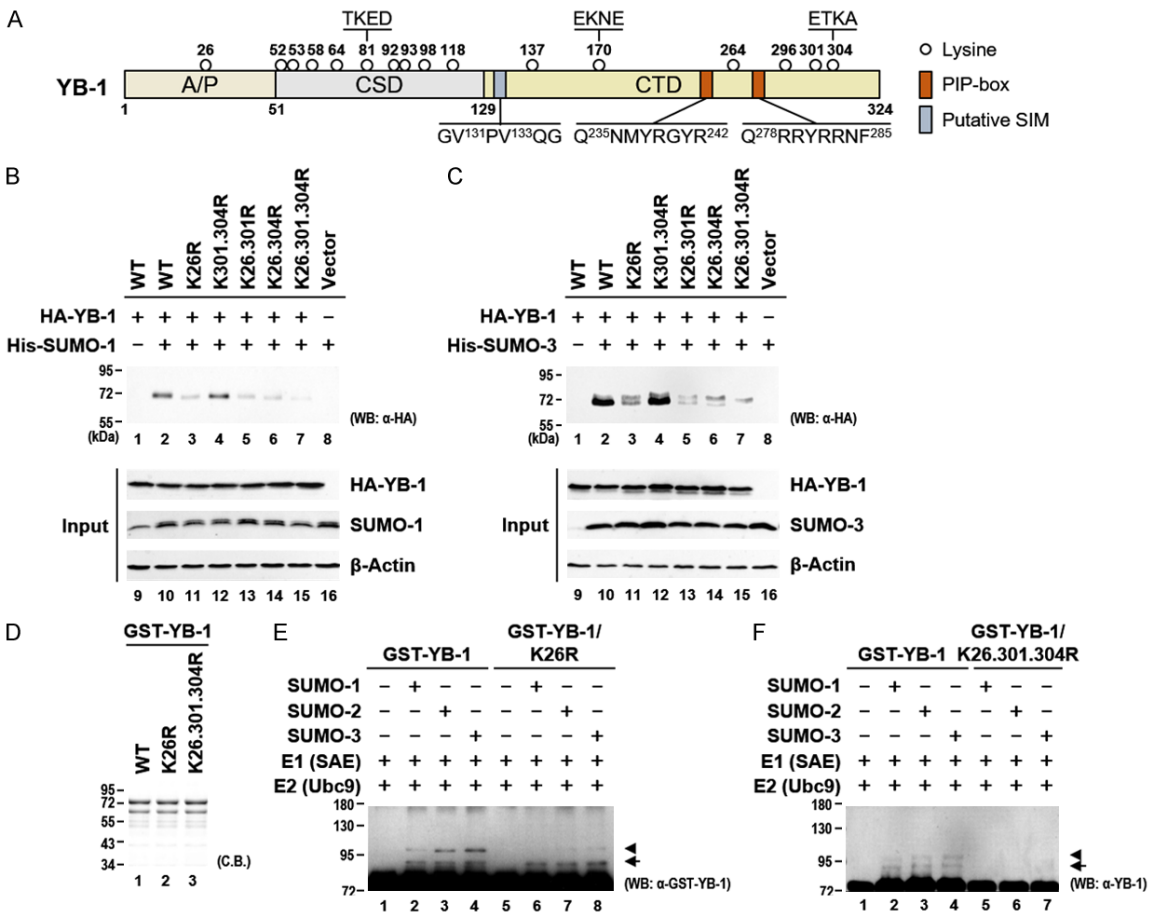

Figure 2. Lys[26] is an important SUMO acceptor lysine residue in YB-1. (A) Schematic diagram of the protein structure of YB-1, which consists of an N-terminal alanine/proline-rich domain (A/P domain), a central cold shock domain (CSD), and a C-terminal domain (CTD). The open circles represent the positions of 16 lysine residues in YB-1. The potential sumoylation sites predicted by GPS-SUMO 1.0 software are shown. The positions and amino acid sequences of the PCNA-interacting protein-box (PIP-box) and the putative SUMO-interacting motif (SIM) are also indicated. (B, C) An *in vivo* sumoylation assay similar to that described in **Figure 1** was carried out with plasmids expressing wild-type HA-YB-1 and its lysine (K)-to-arginine (R) mutants as well as a construct expressing His-SUMO-1 (A) or His-SUMO-3 (B). The expression of transfected proteins in the whole-cell lysates was analyzed by immunoblotting using antibodies against the HA tag, SUMO-1, SUMO-3, and β-actin. β-Actin was used as a loading control. (D) Purified GST, GST-YB-1, GST-YB-1/K26R, and GST-YB-1/K26.301.304R were analyzed by SDS-PAGE and Coomassie brilliant blue (C.B.) staining. (E, F) *In vitro* sumoylation of purified GST-YB-1, GST-YB-1/K26R, and GST-YB-1/K26.301.304R (1 μg/reaction) was carried out with SUMOlink SUMO-1 and SUMO-2/3 Kits. The reaction mixture was resolved by SDS-PAGE and analyzed by western blotting using an anti-GST-YB-1 (E) or anti-YB-1 (F) antibody. Sumoylated GST-YB-1 and its variants are indicated by arrows and arrowheads.

The YB-1/SUMO interaction is important for YB-1 sumoylation

As a typical Ubc9-binding ΨKxD/E motif for SUMO conjugation was not found in YB-1 and the interaction between YB-1 and Ubc9 was not observed in this study (Figure S2), YB-1 might be sumoylated by molecular mechanisms other than direct interaction with Ubc9 [22]. Therefore, we investigated the possibility that YB-1 interacts with SUMO proteins and sought to determine whether this interaction participates in YB-1 sumoylation. To this end, an *in vitro* binding assay was performed using recombinant GST and GST-YB-1 along with His-SUMO-1 or His-SUMO-3, and direct interactions between GST-YB-1 and His-SUMO-1 or SUMO-3 were observed (**Figure 3A**, lane 5). This finding demonstrated that YB-1 directly interacts with SUMO paralogs, implying that YB-1 might possess a SUMO-interacting motif (SIM).

Because no consensus SIM was identified, YB-1 might contain a SIM variant. To delineate

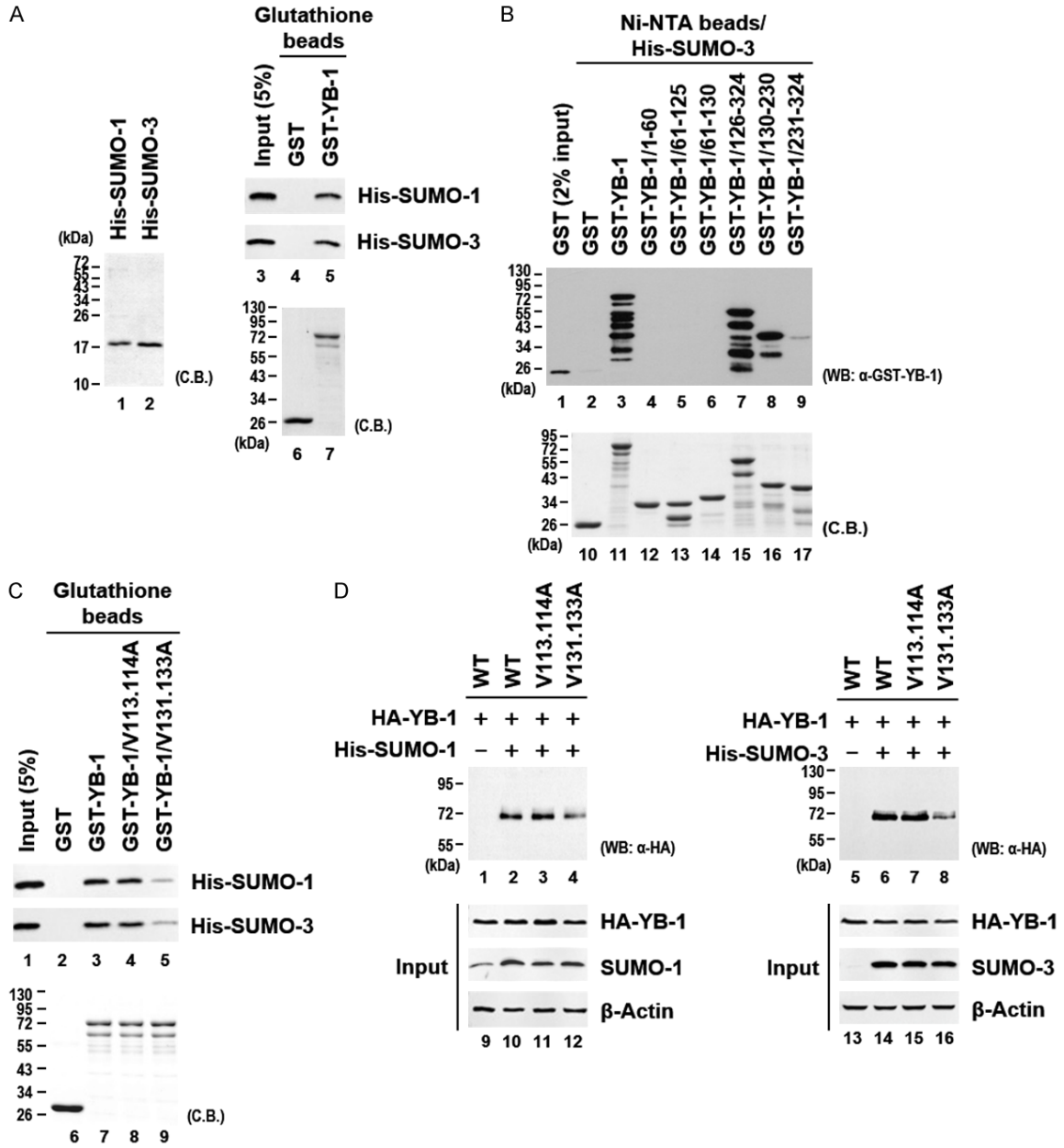

Figure 3. Direct interactions between YB-1 and SUMO proteins contribute to the sumoylation of YB-1. (A) Purified His-SUMO-1, His-SUMO-3, GST, and GST-YB-1 were analyzed by SDS-PAGE and Coomassie brilliant blue (C.B.) staining. An *in vitro* binding assay was performed with glutathione-Sepharose 4B beads-bound GST or GST-YB-1 with His-SUMO-1 or His-SUMO-3. Proteins bound to the beads were analyzed by western blotting using an antibody against SUMO-1 or SUMO-3. (B) An *in vitro* binding assay was carried out with purified GST-YB-1 truncation mutants and His-SUMO-3. Ni-NTA beads were added to isolate GST-YB-1/His-SUMO-3 complexes, and proteins retained on the beads were analyzed by western blotting using an anti-GST-YB-1 antibody. The lower panel shows Coomassie brilliant blue (C.B.) staining of purified proteins. (C) An *in vitro* binding assay similar to that described in (A) was conducted, except purified GST-YB-1/V113.114A, and GST-YB-1/V131.133A were also included. The lower panel shows Coomassie brilliant blue (C.B.) staining of purified proteins. (D) HEK293T cells transfected with plasmids expressing HA-YB-1, HA-YB-1/V113.114A, and HA-YB-1/V131.133A, as well as His-SUMO-1 or His-SUMO-3, were subjected to an *in vivo* sumoylation assay (lanes 1-8). Whole-cell lysates were analyzed by western blotting using antibodies against the HA tag, SUMO-1, SUMO-3, and β-actin to confirm the expression of transfected proteins (lanes 9-16). β-Actin was used as a loading control.

the SUMO-binding region in YB-1, several GST-YB-1 truncation mutants were generated and subjected to an *in vitro* binding assay. As shown in **Figure 3B**, in addition to interacting with full-

length GST-YB-1 (lane 3), His-SUMO-3 interacted with GST-YB-1/126-324 and GST-YB-1/130-230 (lanes 7 and 8), but not with GST (lane 2) or the other GST-YB-1 truncation variants (lanes 4-6 and 9). This result revealed that SUMO-3 associates with YB-1 in the region containing amino acid residues 130-230. Within this YB-1 coding region, a small motif with two valine residues ($GV^{131}PV^{133}QG$) was observed. To explore the importance of this motif in the YB-1/SUMO interaction, the two valine residues in this motif were substituted with alanine to generate the GST-YB-1/V131.133A mutant. Because another motif ($DV^{113}V^{114}EG$) containing two valine residues was located outside this region, the GST-YB-1/V113.114A mutant was also generated as a control in the *in vitro* binding assay. As shown in **Figure 3C**, the binding affinity of GST-YB-1/V131.133A for both His-SUMO-1 and His-SUMO-3 was reduced relative to that of GST-YB-1 (compare lane 5 with lane 3), while that for GST-YB-1/V113.114A was not significantly affected. Thus, the motif containing Val^{131} and Val^{133} is crucial for the YB-1/SUMO interaction.

Next, we examined whether the integrity of the motif containing Val^{131} and Val^{133} is crucial for YB-1 sumoylation by using an *in vivo* sumoylation assay with plasmids expressing HA-YB-1 with the V113.114A and V131.133A mutations. As shown in **Figure 3D**, YB-1/V131.133A was modified by both SUMO-1 and SUMO-3 to a lesser extent than YB-1 (compare lane 4 with lane 2 and lane 8 with lane 6), but this was not the case for YB-1/V113.114A (lanes 3 and 7). These results indicated that the integrity of the Val^{131}/Val^{133}-containing motif of YB-1 is important for its sumoylation.

The subcellular localization, protein stability, and transcriptional regulatory activity of YB-1 are not significantly affected by sumoylation

Post-translational modification provides an efficient and rapid way to change the properties or activity of a target protein, such as alteration in its subcellular localization, protein stability, or function [62, 63]. To determine whether YB-1 sumoylation affects its subcellular localization, plasmids expressing HA-YB-1, HA-YB-1/K26R, HA-YB-1/K301.304R, and HA-YB-1/K26.301.304R were transfected into HeLa cells, which were then subjected to an indirect immunofluorescence assay with an anti-HA antibody. The distribution patterns of these wild-type and mutant YB-1 proteins were similar, as determined by confocal microscopy, and these proteins were localized mainly in the cytoplasm (**Figure 4A**). To investigate whether the protein stability of YB-1 is altered by sumoylation, HeLa cells transfected with the same set of plasmids expressing the wild-type and mutant HA-YB-1 proteins described above were treated with the translation inhibitor cycloheximide for different periods of time. We found that the half-lives of YB-1, YB-1/K26R, and YB-1/K301.304R were similar, ranging from 9.53 to 9.66 h, whereas a slight reduction in the half-life of YB-1/K26.301.304R was observed (8.31 h, **Figure 4B**). In addition, the expression of YB-1 has been reported to be correlated with the expression of *MDR-1* in several cell types [1, 2, 10]. To examine the effect of YB-1 sumoylation on its transcriptional regulatory activity, HeLa cells were co-transfected with a reporter construct containing the *MDR-1* promoter and a plasmid expressing HA-YB-1 or HA-YB-1/K26R. We found that YB-1 and YB-1/K26R exhibited a similar ability to up-regulate *MDR-1* promoter activity (**Figure 4C**). Together, these observations suggested that the reduction in the sumoylation level does not have a significant impact on the subcellular localization, protein stability, and transcriptional regulatory activity of YB-1.

YB-1 sumoylation enhances PCNA binding but inhibits MutSα mismatch binding activity

The protein-protein interaction activity of a target protein might be affected by its sumoylation [62]. Our previous study indicated that YB-1 competes with MutSα for binding to PCNA and inhibits MutSα mismatch binding activity, which leads to MMR deficiency [48]. Next, we examined the possibility that sumoylation of YB-1 plays a role in the regulation of its PCNA binding affinity by using a co-immunoprecipitation assay with cells transiently expressing FLAG-YB-1, FLAG-YB-1/K26R, FLAG-YB-1/K301.304R, and FLAG-YB-1/K26.301.304R (**Figure 5A**). The PCNA-binding activity of YB-1/K301.304R was similar to that of YB-1 (compare lane 4 to lane 2). However, YB-1/K26R showed a lower affinity for PCNA than did YB-1 (lane 3), and a larger reduction in the PCNA binding affinity was further observed for YB-1/

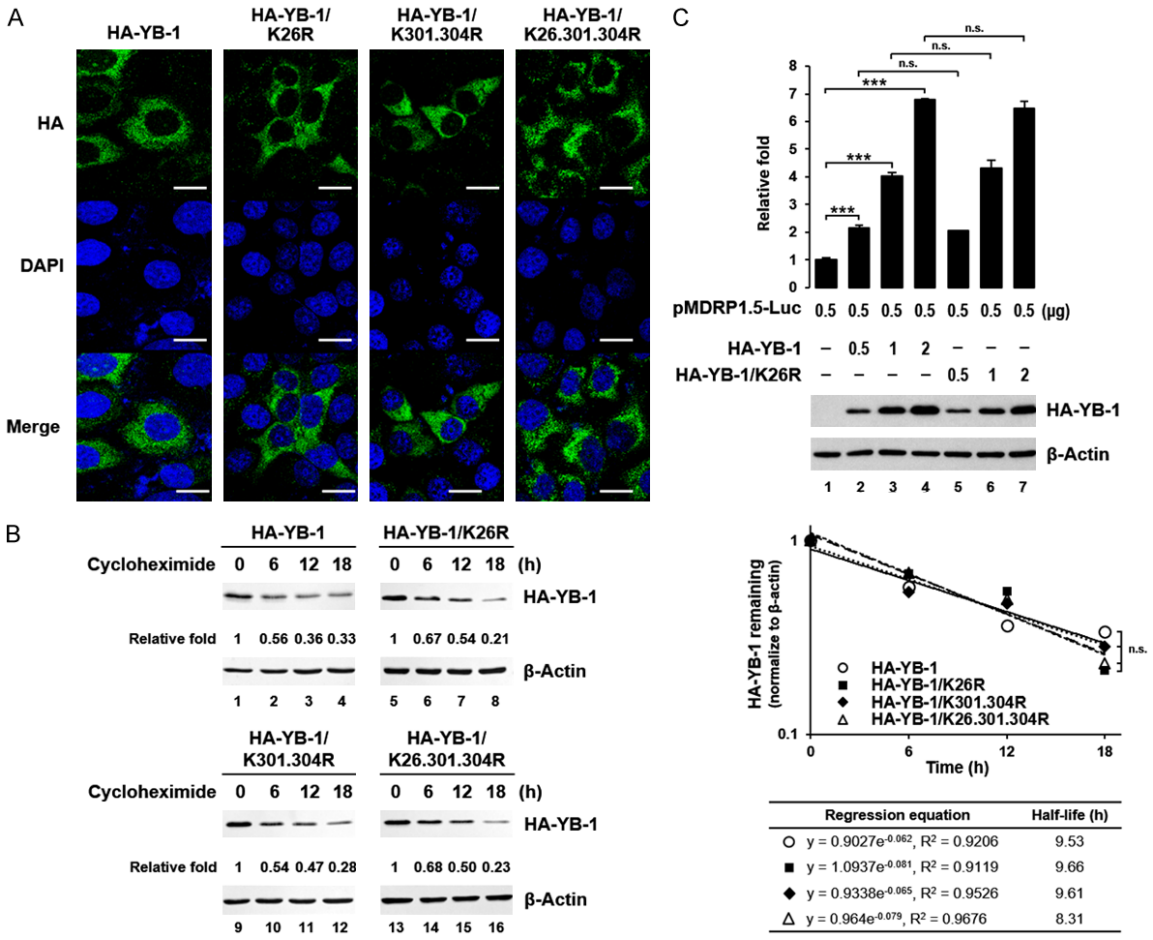

Figure 4. The subcellular localization, protein stability, and transcriptional regulatory activity of YB-1 are not significantly affected by sumoylation. (A) Plasmids expressing HA-YB-1, HA-YB-1/K26R, HA-YB-1/K301.304R, or HA-YB-1/K26.301.304R were transfected into HeLa cells. Forty-eight hours post transfection, the cells were fixed and subjected to an indirect immunofluorescence assay with a mouse anti-HA tag antibody and Alexa Fluor 488-conjugated goat anti-mouse IgG (green). Nuclei were stained with DAPI (blue). Cells were observed under a confocal microscope. The scale bar represents 20 μm. (B) HeLa cells were transfected with plasmids as described in (A) and treated with 100 μg/ml cycloheximide 48 h post transfection. Cells were harvested at the indicated time points after cycloheximide addition, and cellular proteins were analyzed by western blotting with antibodies against the HA tag and β-actin. The protein levels of HA-YB-1 variants were quantified by ImageJ software (National Institutes of Health, Bethesda, MD, USA) and normalized to that of β-actin, and the half-lives of these proteins were determined by regression analysis. The protein levels of HA-YB-1 variants without cycloheximide treatment (0 h) were arbitrarily set as 1. Statistical analyses were carried out using two-way ANOVA (n.s., not significant, $P > 0.05$). (C) pMDRP1.5-Luc was transfected into HeLa cells alone or in combination with different amounts of plasmid expressing HA-YB-1 or HA-YB-1/K26R as indicated. Forty-eight hours post transfection, a luciferase reporter activity assay was performed. The data are presented as the relative fold changes and are derived from at least three independent experiments. The error bars indicate ±1 s.d. of the mean. The same lysates used in the luciferase assay were also subjected to western blotting using antibodies against the HA tag and β-actin. β-Actin was used as a loading control. Statistical analyses were carried out using one-way ANOVA and Tukey's post hoc test (n.s., not significant, $P > 0.05$; ***, $P < 0.001$).

K26.301.304R (lane 5). The PCNA-binding activities of these YB-1 mutants were correlated with their sumoylation levels (**Figure 2**), implying that sumoylation may modulate the interaction between YB-1 and PCNA.

The regulatory role of YB-1 sumoylation in its PCNA-binding activity was further confirmed by a different set of co-immunoprecipitation assays using cell lines with stable overexpression of YB-1 and its mutants. Nuclear extracts of vector control cells (H02) and several HeLa cell lines with stable overexpression of HA-YB-1 (YW86 and YW89), HA-YB-1/K26R (YS53 and YS69), HA-YB-1/K301.304R (YD21 and YD24), and HA-YB-1/K26.301.304R (YT37 and YT38)

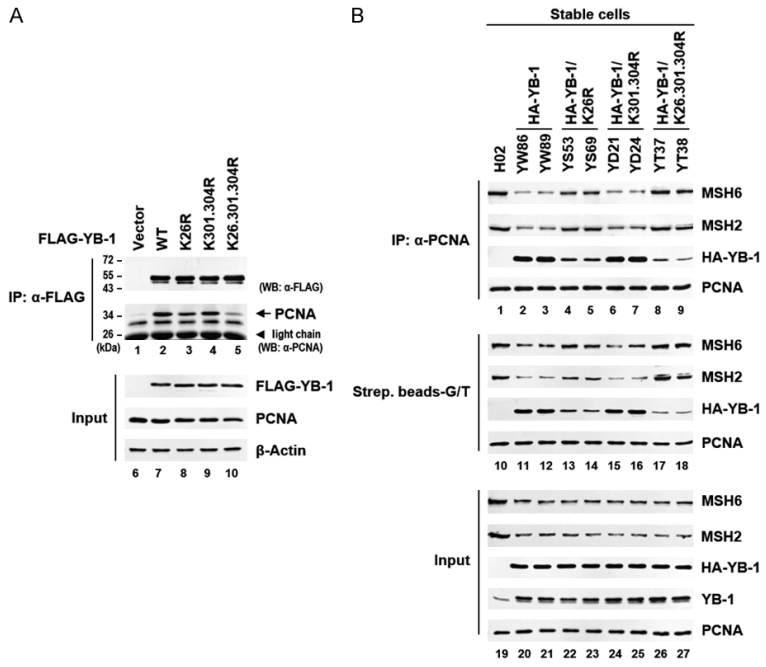

Figure 5. Sumoylation of YB-1 enhances its PCNA-binding activity but inhibits the mismatch binding activity of MutSα. (A) Plasmids expressing FLAG, FLAG-YB-1, FLAG-YB-1/K26R, FLAG-YB-1/K301.304R, or FLAG-YB-1/K26.301.304R were transfected into HEK293T cells. Whole-cell lysates were prepared 48 h post transfection and subjected to a co-immunoprecipitation assay with anti-FLAG M2 magnetic beads. Proteins bound to the beads were analyzed by western blotting using antibodies against the FLAG tag and PCNA (lanes 1-5). Co-immunoprecipitated PCNA is indicated by an arrow. The arrowhead indicates the position of the IgG light chain. Protein expression in cells was determined by western blotting with anti-FLAG, anti-PCNA, and anti-β-actin antibodies (lanes 6-10). β-Actin was used as a loading control. (B) Nuclear extracts of vector control cells (H02) and several cell lines with stable overexpression of HA-YB-1 (YW86 and YW89), HA-YB-1/K26R (YS53 and YS69), HA-YB-1/K301.304R (YD21 and YD24), or HA-YB-1/K26.301.304R (YT37 and YT38) were prepared and subjected to the following experiments. For the co-immunoprecipitation assay, nuclear extracts of these cells were incubated with an anti-PCNA antibody and protein G-Sepharose beads (lanes 1-9). For the biotinylated DNA pull-down assay (lanes 10-18), nuclear extracts of these cells were incubated with streptavidin beads-bound biotinylated G/T heteroduplexes (50 pmol). Proteins retained on the beads were analyzed by western blotting with antibodies against MSH6, MSH2, the HA tag, and PCNA. Protein expression in nuclear extracts was evaluated with antibodies against MSH6, MSH2, the HA tag, YB-1, and PCNA (lanes 19-27).

were subjected to a co-immunoprecipitation assay with an anti-PCNA antibody. Consistent with our observation described above (**Figure 5A**), YB-1/K26R and YB-1/K26.301.304R exhibited lower affinities for PCNA than did YB-1 (**Figure 5B**, compare lanes 4-5 and lanes 8-9 with lanes 2-3), suggesting that a decreased level of YB-1 sumoylation diminished its interaction with PCNA. Moreover, abolishing YB-1 sumoylation not only inhibited the interaction between PCNA and YB-1 but also compromised the YB-1-mediated interference with the formation of the MutSα (MSH2/MSH6 heterodimer)/PCNA complex, as the binding of MSH2 and MSH6 to PCNA was significantly stronger in the presence of the K26R or K26.301.304R mutant than in the presence of wild-type YB-1 (**Figure 5B**, compare lanes 4-5 and lanes 8-9 with lanes 2-3). Considering that the mismatch recognition activity of MutSα can be enhanced by its interaction with PCNA, our results implied that YB-1 sumoylation may potentiate YB-1-mediated inhibition of the binding of MutSα to mismatches. This idea was further supported by the results from the biotinylated DNA pull-down assay (**Figure 5B**, lanes 10-18). MutSα/PCNA complex formation on the biotinylated G/T heteroduplex was suppressed in YB-1-overexpressing cells compared to control cells (compare lanes 11-12 with lane 10), but this inhibitory effect was counteracted in cells overexpressing YB-1/K26R (lanes 13-14) or YB-1/K26.301.304R (lanes 17-18). These results indicated that sumoylation of YB-1 is important for its interaction with PCNA and its inhibition of the mismatch binding activity of MutSα.

Sumoylation of YB-1 increases the spontaneous mutation frequency

MMR is coupled with DNA replication to reduce the occurrence of mutations and protect cells from acquiring the mutator phenotype, whereas defects in MMR activity result in genomic instability with a signature of enhanced spontaneous mutation [33, 36, 37]. In our previous study, YB-1 was found to interact with PCNA to reduce the mismatch binding activity of MutSα,

which led to MMR deficiency with the phenotype of an increased spontaneous mutation frequency [48]. As decreased YB-1 sumoylation impaired its PCNA binding affinity and compromised YB-1-mediated disruption of MutSα/PCNA complex formation (**Figure 5**), sumoylation of YB-1 may be involved in the regulation of YB-1-mediated genomic instability. To test this hypothesis, the spontaneous mutation frequency was analyzed by an ouabain resistance assay as previously described [48]. Mutations in the gene encoding the Na^+/K^+ ATPase α1 subunit lead to amino acid substitutions, which protect cells from killing by the Na^+/K^+ ATPase inhibitor ouabain and facilitate colony formation under ouabain selection [64, 65]. In this study, vector control and several HeLa cell lines with stable overexpression of HA-YB-1, HA-YB-1/K26R, HA-YB-1/K301.304R, and HA-YB-1/K26.301.304R were used in the ouabain resistance assay (**Figure 6A**). We found that the percentages of ouabain-resistant colonies formed by YB-1-overexpressing cells (YW86 and YW89) were ~21- to 24.7-fold higher than those formed by vector control cells (H02), consistent with the results of our previous study [48]. Moreover, the enhancement of ouabain resistance in YB-1/K301.304R-overexpressing cells (YD21 and YD24, ~21.3- to 23-fold increase) was similar to that in YB-1-overexpressing cells. However, the number of ouabain-resistant colonies formed by cells overexpressing YB-1/K26R (YS53 and YS69, ~10- to 11-fold increase) or YB-1/K26.301.304R (YT37 and YT38, ~4- to 4.7-fold increase) was much lower than that formed by wild-type YB-1-overexpressing cells, suggesting that sumoylation plays a positive role in YB-1-mediated accumulation of spontaneous mutations and genomic instability.

YB-1 sumoylation enhances alkylator tolerance upon MNNG treatment

As discussed in the Introduction section, treating MMR-proficient, low-MGMT cells with the S_N1-type mono-functional alkylator MNNG activates the MMR-dependent DNA damage response via two proposed mechanisms described by the "futile repair cycle" and "direct signaling" models, thereby inducing cell cycle arrest, apoptosis, and cell death [49-51]. YB-1 prevents MutSα from binding to mismatches [48], and YB-1 sumoylation may play a functional role in MMR deficiency (**Figures 5** and **6A**), raising the possibility that MNNG-induced cytotoxicity might be affected by YB-1 and its sumoylation. A previous report indicates that treating cells with a high concentration of MNNG induces MMR-independent DNA damage [66]. Thus, in this study, MMR-proficient HeLa cells were treated with the MGMT inhibitor O^6-benzylguanine (25 μM) and a low concentration (0.05 μM) of MNNG. In the presence of O^6-benzylguanine, the level of MGMT was significantly decreased and MNNG-induced cytotoxicity was enhanced in HeLa cells (Figure S3). To investigate the impact of YB-1 and its sumoylation on regulating MNNG-induced cytotoxicity, the vector control and several HeLa cell lines with stable overexpression of wild-type and mutant HA-YB-1, as described above, were treated with MNNG and O^6-benzylguanine and subjected to a colony formation assay (**Figure 6B** and **6C**). Upon MNNG treatment, cells overexpressing YB-1 (YW86 and YW89) and YB-1/K301.304R (YD21 and YD24) exhibited ~8.8- to 9.5-fold higher alkylator tolerance than vector control cells, while cells overexpressing YB-1/K26R (YS53 and YS69, ~3.7- to 4.2-fold increase) and YB-1/K26.301.304R (YT37 and YT38, ~2.5- to 2.8-fold increase) showed higher susceptibility to MNNG-induced cytotoxicity than wild-type YB-1-overexpressing cells. These results indicated that YB-1 can promote the development of alkylator tolerance in cancer cells and that sumoylation is critical for YB-1 to inhibit cell susceptibility to alkylator insult.

YB-1 and its sumoylation inhibit MNNG-induced cell cycle arrest and apoptosis

Next, we elucidated the role of YB-1 and its sumoylation in MNNG-induced G2/M-phase arrest and apoptosis. To this end, the unsynchronized vector control cells (H02) and HeLa cells with stable overexpression of HA-YB-1 (YW89) and YB-1/K26R (YS53) were treated with MNNG and O^6-benzylguanine. After MNNG treatment, cells were harvested every 12 h until the 84 h time point and the DNA content was then measured by flow cytometry to analyze the cell cycle phase distribution (**Figure 7**). We found that the cell cycle profiles of these cells within the first 24 h were similar and that the cells exhibited normal cell cycle phase distributions. After 36 h of MNNG treatment, the population of cells with G2/M-phase was increased. Interestingly, overexpression of YB-1

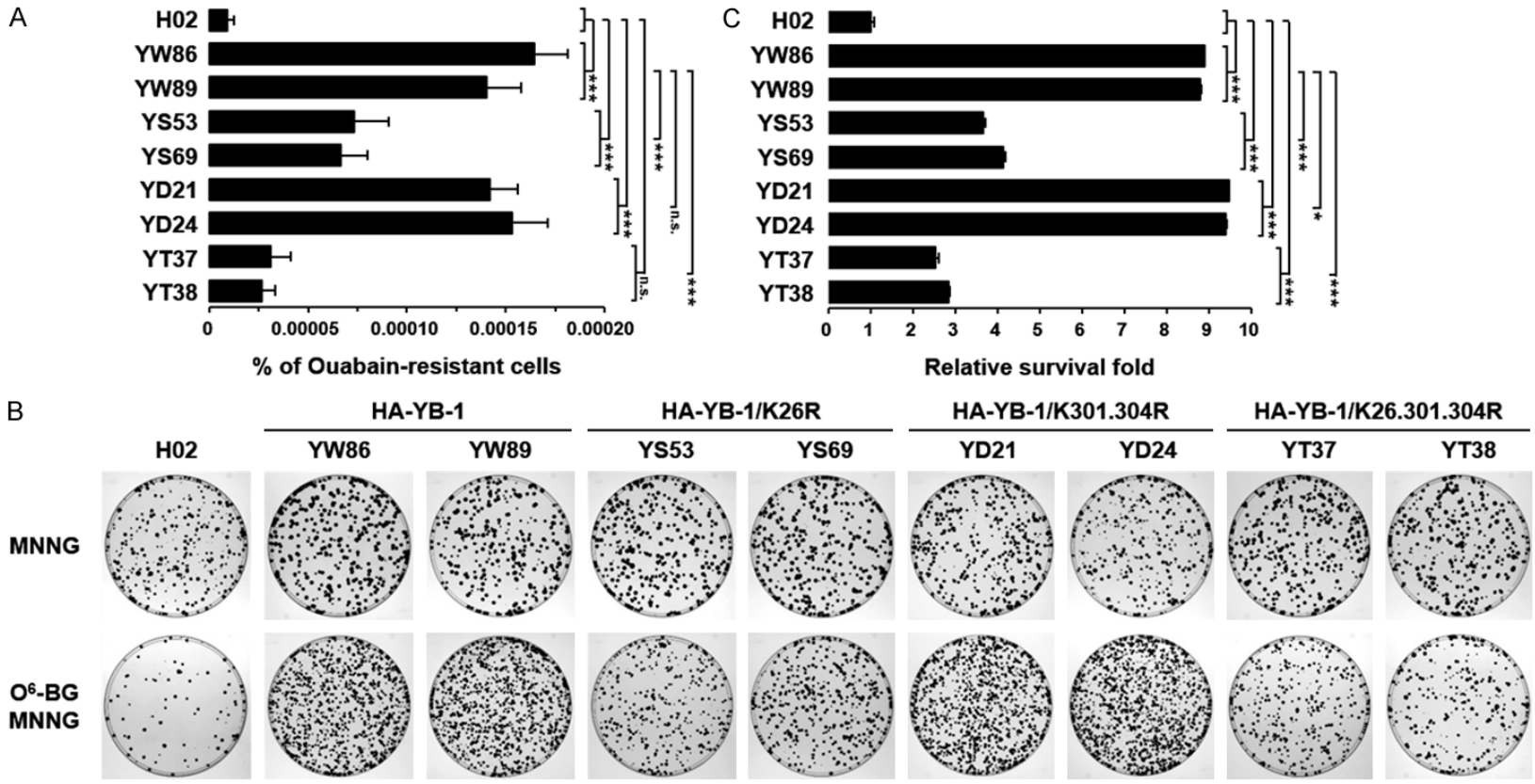

Figure 6. YB-1 sumoylation increases spontaneous mutations in the *Na^+/K^+ ATPase α1 subunit* and protects cells against MNNG-induced cytotoxicity. (A) Vector control cells (H02) and several cell lines with stable overexpression of HA-YB-1 (YW86 and YW89), HA-YB-1/K26R (YS53 and YS69), HA-YB-1/K301.304R (YD21 and YD24), or HA-YB-1/K26.301.304R (YT37 and YT38) (~3 × 10^7 cells each) were subjected to an ouabain resistance assay. Cells were seeded (10^6 cells/10-cm dish) and selected with complete medium containing 7.5 × 10^{-2} μM ouabain. In addition, the relative clonogenic frequency of these cells was examined by seeding ~300 cells per 10-cm dish in nonselective medium. After incubation for 10-14 days, the number and percentage of ouabain-resistant colonies were determined and calculated, respectively. The results were derived from three independent experiments, and the error bars indicate ±1 s.d. of the mean. Statistical analyses were carried out using one-way ANOVA and Tukey's post hoc test (n.s., not significant, $P > 0.05$; ***, $P < 0.001$). (B) Vector control cells and cells with stable overexpression of wild-type or mutant HA-YB-1 described in (A) were incubated in complete medium with or without 25 μM O^6-benzylguanine (O^6-BG), treated with 0.05 μM MNNG, reseeded in 10-cm dishes, and subjected to a colony formation assay. For cells treated only with MNNG, ~300 cells per 10-cm dish were reseeded, and for MNNG/O^6-benzylguanine-treated cells, ~1200 cells per 10-cm dish were reseeded. (C) The surviving colonies shown in (B) were counted, and the numbers of MNNG/O^6-benzylguanine-treated cell colonies were normalized to those of MNNG-treated cells. The survival rates of cells with stable overexpression of wild-type or mutant HA-YB-1 were normalized to that of H02 cells. The results were derived from three independent experiments, and the error bars indicate ±1 s.d. of the mean. Statistical analyses were carried out using one-way ANOVA and Tukey's post hoc test (n.s., not significant, $P > 0.05$; *, $P < 0.05$; ***, $P < 0.001$).

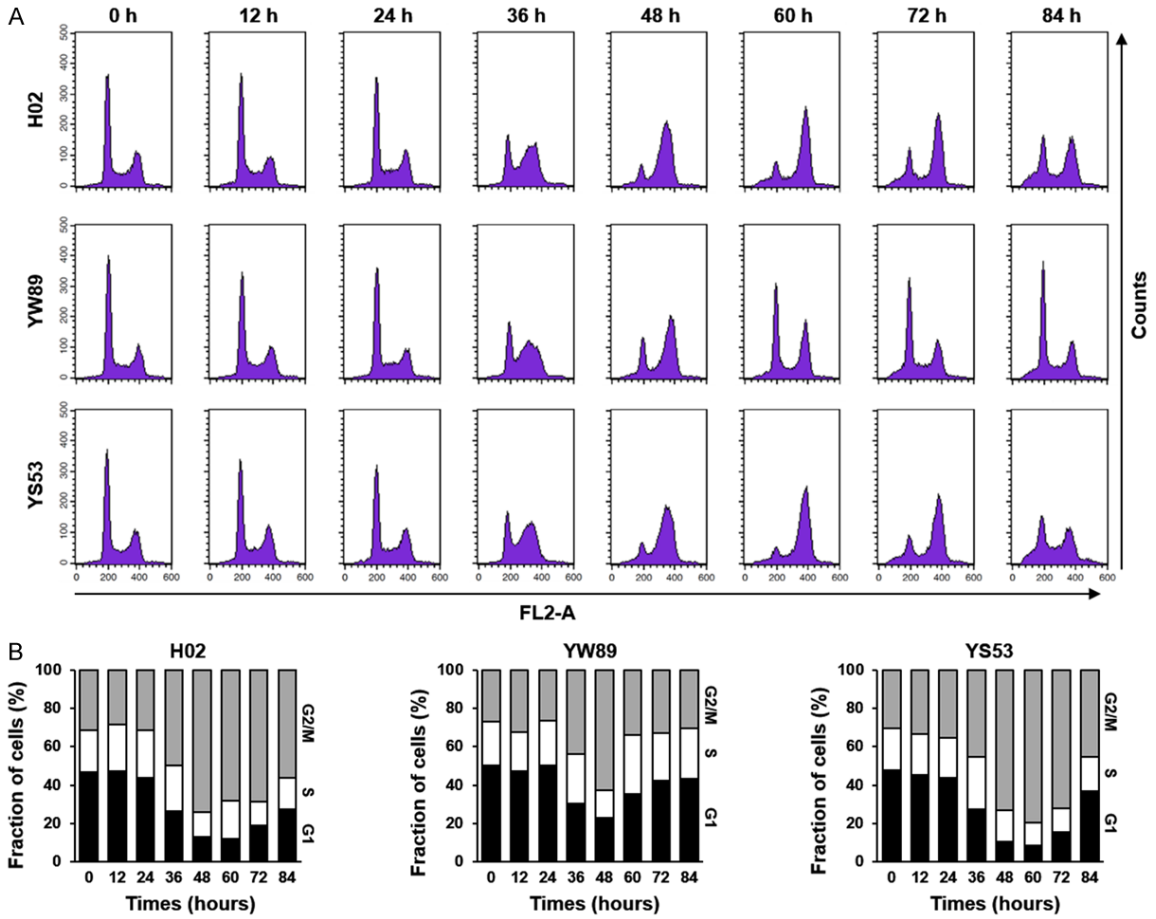

Figure 7. YB-1 and its sumoylation are involved in early escape from G2/M-phase arrest upon MNNG treatment. (A) Vector control cells (H02) as well as cells with stable overexpression of HA-YB-1 (YW89) or HA-YB-1/K26R (YS53) were treated with 0.05 μM MNNG for 3 h in the presence of 25 μM O^6-benzylguanine. Cells were harvested at the indicated time points, fixed with ethanol, stained with propidium iodide, and subjected to flow cytometric analysis of the DNA content by using a FACSCalibur flow cytometer (BD Biosciences). (B) Histogram of the cell cycle (G1, S, and G2/M) phase distribution in H02, YW89, and YS53 cells at different time points.

(YW89) promoted the early escape of cells from MNNG-induced G2/M-phase arrest, and this effect was compromised by disruption of Lys^{26} sumoylation (YS53). In addition, the effects of YB-1 and its sumoylation on MNNG-induced apoptosis in H02, YW89, and YS53 cells at 96 h after MNNG and O^6-benzylguanine treatment were investigated by using Annexin V staining (**Figure 8A**). Apoptosis (15.24%) was observed in vector control cells (H02) after 96 h of MNNG treatment. However, overexpression of YB-1 (YW89) decreased MNNG-induced apoptosis (6.25%), whereas loss of Lys^{26} sumoylation of YB-1 (YS53) impaired this protection (11.7% apoptosis rate). These findings suggested that YB-1 and its sumoylation play critical roles in protecting cells from MNNG-induced cell cycle arrest and apoptosis, which may contribute to the development of an alkylator-tolerant phenotype in YB-1-overexpressing cells.

YB-1 and its sumoylation suppress MMR-dependent DNA damage signaling

As described above, sumoylation of YB-1 is involved in the inhibition of MNNG-induced G2/M-phase arrest (**Figure 7**), implying that YB-1 sumoylation may suppress MMR-dependent DNA damage response signaling after alkylator insult. To verify this hypothesis, vector control cells (H02) and HeLa cell lines with stable overexpression of HA-YB-1 (YW89) and HA-YB-1/K26R (YS53) were treated with MNNG in the presence of O^6-benzylguanine, and the cells were harvested 24, 48, and 72 h after MNNG treatment (**Figure 8B**). The protein levels

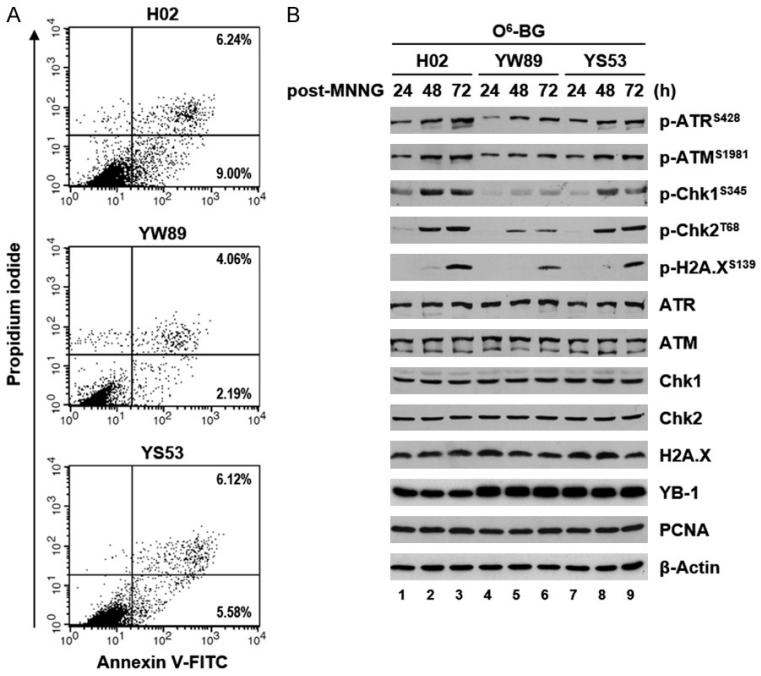

Figure 8. YB-1 and its sumoylation play important roles in YB-1-mediated inhibition of apoptosis and MMR-dependent DNA damage response signaling upon MNNG treatment. (A) Vector control cells (H02) as well as cells with stable overexpression of HA-YB-1 (YW89) or HA-YB-1/K26R (YS53) were treated with 0.05 μM MNNG for 3 h in the presence of 25 μM O^6-benzylguanine. The cells were harvested 96 h after MNNG treatment and stained with propidium iodide and Annexin V-FITC to quantitatively analyze the apoptotic population by using a FACSCalibur flow cytometer (BD Biosciences). The apoptotic population is localized in the upper right and lower right quadrants, and the percentage of cells in each quadrant is summarized in each panel. (B) Vector control cells (H02) as well as cells with stable overexpression of HA-YB-1 (YW89) or HA-YB-1/K26R (YS53) were treated with 0.05 μM MNNG for 3 h in the presence of 25 μM O^6-benzylguanine (O^6-BG). Whole-cell extracts were prepared at the indicated time points after MNNG treatment and analyzed by western blotting using antibodies against phospho-ATR^{Ser428}, phospho-ATM^{Ser1981}, phospho-Chk1^{Ser345}, phospho-Chk2^{Thr68}, phospho-H2A.X^{Ser139}, ATR, ATM, Chk1, Chk2, H2A.X, YB-1, PCNA, and β-actin. β-Actin was used as a loading control.

of ATR, ATM, Chk1, Chk2, γ-H2A.X, YB-1, and PCNA were analyzed by western blotting. The phosphorylation status of ATR, ATM, Chk1, Chk2, and γ-H2A.X was also evaluated. We found that the phosphorylation of ATR, ATM, Chk1, Chk2, and γ-H2A.X was decreased in HA-YB-1-overexpressing cells (YW89, lanes 4-6) compared to vector control cells (H02, lanes 1-3) after MNNG treatment, although this suppressive effect was not as significant as that in HA-YB-1/K26R-overexpressing cells (YS53, lanes 7-9). This observation suggested that sumoylation may play an important role in potentiating the inhibitory activity of YB-1 toward the MMR-dependent DNA damage response.

Discussion

In this study, our results indicated that YB-1 is a target protein of the sumoylation pathway (**Figure 1**) and that Lys^{26} is an important SUMO acceptor lysine residue in YB-1 (**Figure 2**). We found that YB-1 directly interacts with SUMO proteins and that amino acid substitutions of Val^{131} and Val^{133} in the putative SIM of YB-1 reduced its sumoylation level (**Figure 3**). Although the subcellular localization, protein stability, and transcriptional regulatory activity of YB-1 were not significantly affected (**Figure 4**), the PCNA binding affinity of YB-1 was enhanced by sumoylation (**Figure 5A**). Sumoylated YB-1 more efficiently competed with MutSα for binding to PCNA and inhibited the mismatch binding activity of MutSα (**Figure 5B**). Disruption of the MutSα/PCNA interaction by YB-1 and its sumoylation resulted in the enhancement of spontaneous mutation and resistance to MNNG-induced cell death (**Figure 6**). In addition, sumoylation of YB-1 reduced MNNG-mediated cytotoxicity by inducing early escape from G2/M-phase arrest, inhibiting apoptosis, and suppressing the MMR-dependent DNA damage response (**Figures 6-8**). Taken together, these findings indicate that YB-1 sumoylation plays functional roles in the induction of MMR deficiency, which contributes to YB-1-mediated tumorigenesis and alkylator tolerance (**Figure 9**).

To explain the molecular process of sumoylation at a SUMO acceptor lysine residue in a target protein, three mechanisms have been delineated [22]. First, target proteins possess a consensus ΨKxD/E motif for direct binding to the SUMO-conjugating enzyme Ubc9 (E2); second, target proteins contain a SIM for direct interaction with SUMO proteins; third, for proteins without a ΨKxD/E motif and SIM, a direct inter-

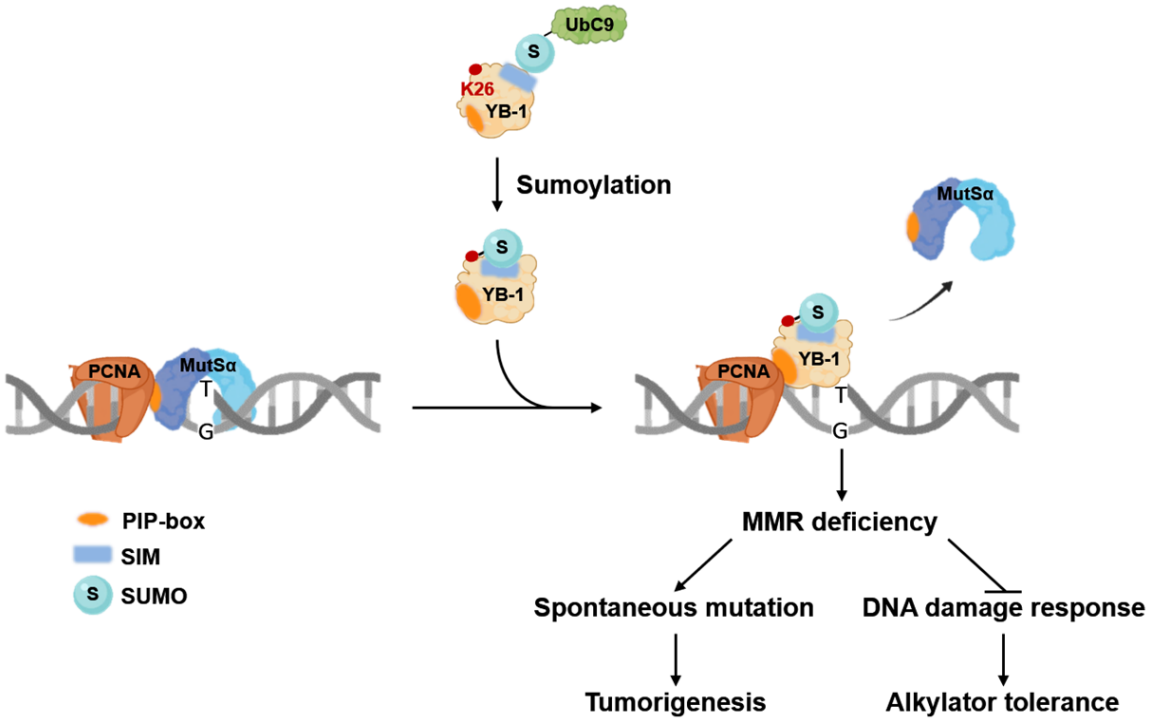

Figure 9. A proposed model showing that sumoylation is involved in the modulation of YB-1-induced MMR deficiency and alkylator tolerance. YB-1 is sumoylated through its direct interaction with SUMO proteins at the SIM in YB-1. The intramolecular interaction between a SUMO protein and the SIM may result in a conformational change in YB-1, which facilitates the YB-1/PCNA interaction, results in competition with MutSα for PCNA binding, prevents MutSα from binding to mismatches, and induces MMR deficiency. Thus, sumoylation plays functional roles in the YB-1-mediated enhancement of spontaneous mutation and inhibition of the MMR-dependent DNA damage response, which is associated with tumorigenesis and alkylator tolerance in YB-1-overexpressing cells.

action between the target protein and a specific SUMO E3 ligase is important. These models for sumoylation on specific target proteins are not mutually exclusive [22]. In this study, instead of a consensus ΨKxD/E motif, a small motif with two valine residues ($GV^{131}PV^{133}QG$) was found in YB-1, and this motif was found to play an important role in the direct interaction of YB-1/SUMO proteins and YB-1 sumoylation (**Figure 3**). Therefore, YB-1 might be modified by SUMO proteins through a molecular mechanism, as described above in the second model. However, when the sumoylation status of YB-1 was examined with a relatively simple *in vitro* assay system containing purified GST-YB-1, E1, E2, and SUMO proteins, we found that the level of YB-1 sumoylation was non-significant. This finding is consistent with the conclusion that the interaction between the SIM and SUMO proteins is weak [28, 29]. Thus, one or more SUMO E3 ligases must be involved in the process of YB-1 sumoylation *in vivo*.

YB-1 is a highly conserved protein and consists of three major domains: the N-terminal alanine/proline-rich domain (A/P domain), central evolutionarily conserved cold shock domain (CSD), and C-terminal domain (CTD) (**Figure 2A**) [1]. Evidence implies that zebrafish YB-1 (zfYB-1) is a target of the sumoylation pathway [16], but the important lysine residue(s) for SUMO conjugation of zfYB-1 remain unclear. The zfYB-1 and human YB-1 share ~67% amino acid sequence similarity [1]; however, the central CSD of these two species is 100% conserved, and the homology of the A/P domain and the CTD is relatively low [16]. Using GPS-SUMO 1.0 software, two atypical ($TK^{61}ED$ in the CSD and $EK^{152}RE$ in the CTD) sumoylation sites and one inverted ($DSK^{289}A$ in the CTD) sumoylation site were predicted in zfYB-1 [16]. In this study, the potential sumoylation site in human YB-1 was analyzed by the same software, and two non-canonical ($TK^{81}ED$ and $EK^{170}NE$) sumoylation sites and one inverted ($ETK^{304}A$) sumoylation site were found, very similar to zfYB-1.

Nonetheless, we found that the sumoylation levels of human YB-1 mutants with lysine-to-arginine substitutions at these predicted sumoylation sites were not diminished (Figure S1A). Our results indicated that Lys^{26} plays a major role in human YB-1 sumoylation (**Figures 2** and S1A). As the A/P domain of zfYB-1 is shorter than that of human YB-1 and this region contains no lysine residues, the SUMO acceptor lysine residue(s) in zfYB-1 remain to be identified. In addition, the putative SIM ($GV^{131}PV^{133}QG$) in human YB-1 is conserved in zfYB-1 ($GV^{111}PV^{113}QG$), implying that zfYB-1 sumoylation might be partially mediated by a molecular mechanism involving a direct interaction of zfYB-1 with a SUMO protein.

Several SIM-containing proteins preferentially interact with specific SUMO paralog, thereby resulting in paralog-specific sumoylation of these proteins [19, 28, 29]. For example, as the SIM of USP25 binds more strongly to SUMO2/3, it is more efficiently conjugated by SUMO-2/3 [31]. A more complicated illustration demonstrates that phosphorylation in the SIM of Daxx enhances its specific binding to SUMO-1 but has a lesser effect on its binding to SUMO-2/3, thereby resulting in selective sumoylation of Daxx by SUMO-1 and enhancing the interaction of Daxx with SUMO-1-modified cellular factors [67]. In this study, the binding affinity of YB-1 for SUMO-1 and SUMO-3 was similar (**Figure 3A** and **3C**), suggesting that the paralog specificity of the YB-1 SIM is non-significant. The differential levels of YB-1 sumoylation by different SUMO paralogs observed in the *in vivo* sumoylation assay (**Figure 1B**) might partially result from distinct exogenous expression patterns of these SUMO paralogs. Moreover, although there are many YB-1 interaction partners, the SIM of YB-1 may increase the number by interacting with sumoylated proteins, which may play specific roles in the pleiotropic function of YB-1.

The consequences of sumoylation are diverse. Substantial evidences indicate that sumoylation or the presence of a SIM changes the biological properties of proteins, including their stability, subcellular localization, and interactions with cellular factors [22, 23, 28, 29]. In addition to the intermolecular associations of SIM-containing proteins with SUMO or sumoylated factors, intramolecular SUMO-SIM interactions have also been reported. Thymidine DNA glycosylase (TDG) in base excision repair (BER) is the most notable example. Sumoylation induces an intramolecular interaction of SUMO with the SIM of TDG, resulting in a conformational change in TDG and the release of TDG from abasic site to sustain BER process [68-70]. Our previous study demonstrated that YB-1 interacts with PCNA through two PIP-boxes (Q^{235}NMYRGYR^{242} and Q^{278}RRYRRNF^{285}) in the C-terminal region of YB-1 [48]. In the present study, we found that the putative SIM of YB-1 is important for its sumoylation (**Figure 3**), which plays a crucial role in the interaction between YB-1 and PCNA (**Figure 5A**). Therefore, in addition to the PIP-boxes, the SIM of YB-1 also contributes to the YB-1/PCNA interaction. We proposed that, similar to the intramolecular interaction of SUMO with the SIM in TDG, sumoylated YB-1 may undergo structural rearrangement through an intramolecular SUMO-SIM interaction, which may act cooperatively with the PIP-boxes in YB-1 to enhance PCNA binding (**Figure 9**). Thus, the SIM and sumoylation of YB-1 are crucial for disruption of the MutSα/PCNA interaction, the inhibition of MutSα mismatch binding activity, and the increase in the spontaneous mutation frequency.

S_N1-type mono-functional alkylators, including dacarbazine, temozolomide, and MNNG, mainly modify guanine at the N^7 and O^6 positions, adenine at N^1 and N^3 positions, and cytosine at N^3 position [49, 52]. The dominant adducts, N-methylated adenine and guanine, are efficiently repaired by BER or nucleotide excision repair [49]. Although accounting for less than 8% of total methylation modifications, O^6-meG is the most mutagenic and cytotoxic DNA adduct, as MGMT is a suicide enzyme that limits its detoxification capacity [49, 50, 52]. During DNA replication, recognition of O^6-meG:T (thymine) by MutSα initiates MMR, but the mispairing nature of O^6-meG results in the re-incorporation of thymine. These iterative rounds of MMR lead to single-stranded gaps causing replication fork collapses and DNA double-strand breaks during the next DNA replication cycle. In this so-called “futile repair cycle” model, both MMR and DNA replication are required to trigger DNA damage response signaling and to induce cell cycle arrest as well as cell death. An alternative “direct signaling” model, in which the recognition of O^6-meG:T by

MutSα activates ATR-Chk1 signaling to induce cell death, has also been proposed. These two models are not mutually exclusive [32, 49-51, 53]. Given that MutSα recognition of O^6-meG:T is essential for triggering the DNA damage response in these models, MMR acts as a damage sensor to induce cell death upon alkylator insult [32, 49, 51-54]. Our previous study revealed that YB-1 competes with MutSα for binding to PCNA and inhibits MMR activity [48]. In the current study, we found that sumoylation of YB-1 is important for its interaction with PCNA and participates in YB-1-mediated MMR deficiency (**Figures 5**, **6A**). Thus, YB-1 and its sumoylation might play functional roles in the regulation of MNNG-induced cytotoxicity. Our observations in this study support this idea. Overexpression of YB-1 induces the development of alkylator tolerance in cancer cells, and YB-1 sumoylation is important for suppressing cell susceptibility to alkylator insult (**Figure 6B**, **6C**). Moreover, YB-1 and its sumoylation play functional roles in protecting cells from cell cycle arrest, inhibiting apoptosis, and suppressing MMR-dependent DNA damage signaling induced by MNNG (**Figures 7**, **8**), all of which may contribute to the development of an alkylator-tolerant phenotype in YB-1-overexpressing cells.

The enhanced expression of YB-1 has been observed in several kinds of cancers, including breast, ovarian, lung, liver, brain, and colorectal cancers [1, 6, 9-11]. MMR-deficient tumors exhibit alkylator tolerance with increased cell viability and accumulation of mutations after alkylator-based chemotherapy, which results in the poor prognosis of patients with these tumors [49, 51-54]. In this study, we found that YB-1 sumoylation enhances its PCNA binding affinity, which in turn leads to more effective inhibition of the MutSα/PCNA interaction and the mismatch binding activity of MutSα (**Figure 5**). Therefore, YB-1 sumoylation participates in the induction of MMR deficiency and alkylator tolerance (**Figures 6**-**8**). These results will be informative for future research on YB-1-mediated tumorigenesis and the development of a therapeutic strategy for alkylator-tolerant cancers with YB-1 overexpression.

Acknowledgements

We appreciate Dr. Yan-Hwa Wu Lee for critical comments and suggestions on this work. We are grateful to Dr. Pei-Ching Chang for kindly providing the SUMOlink SUMO-1 and SUMO-2/3 Kits. This work was financially supported in part by grants from the Taiwan Ministry of Science and Technology (MOST 107-2320-B-009-006-MY2 and MOST 109-2320-B-009-002 to R.T. Mai; MOST 107-2628-B-009-002, MOST 108-2628-B-009-002, and MOST 109-2628-B-009-004 to C.H. Chao). This work was also financially supported in part by the "Center for Intelligent Drug Systems and Smart Bio-devices (IDS^2B)" and "Smart Platform of Dynamic Systems Biology for Therapeutic Development" from The Featured Areas Research Center Program within the framework of the Higher Education Sprout Project of the Ministry of Education (MOE) in Taiwan. This work was also supported in part by the Higher Education Sprout Project of National Yang Ming Chiao Tung University and the Ministry of Education (MOE) in Taiwan. This work was supported in part by the Artificial Intelligence to Precision Health: Integrating Dynamic Physiological Signals and EMR to Build a Medical Digital Twins Platform sponsored by the Taiwan Ministry of Science and Technology under grant number MOST 111-2321-B-A49-010.

Disclosure of conflict of interest

None.

Address correspondence to: Dr. Ru-Tsun Mai, Department of Biological Science and Technology, College of Biological Science and Technology, National Yang Ming Chiao Tung University, 75 Bo-Ai Street, Hsinchu 300, Taiwan. Tel: +886-3-5712121#56995; Fax: +886-3-5729288; E-mail: mairt@nycu.edu.tw

References

[1] Eliseeva IA, Kim ER, Guryanov SG, Ovchinnikov LP and Lyabin DN. Y-box-binding protein 1 (YB-1) and its functions. Biochemistry (Mosc) 2011; 76: 1402-1433.

[2] Lyabin DN, Eliseeva IA and Ovchinnikov LP. YB-1 protein: functions and regulation. Wiley Interdiscip Rev RNA 2014; 5: 95-110.

[3] Mordovkina D, Lyabin DN, Smolin EA, Sogorina EM, Ovchinnikov LP and Eliseeva I. Y-box binding proteins in mRNP assembly, translation, and stability control. Biomolecules 2020; 10: 591.

[4] Suresh PS, Tsutsumi R and Venkatesh T. YBX1 at the crossroads of non-coding transcriptome,

exosomal, and cytoplasmic granular signaling. Eur J Cell Biol 2018; 97: 163-167.
[5] Lasham A, Print CG, Woolley AG, Dunn SE and Braithwaite AW. YB-1: oncoprotein, prognostic marker and therapeutic target? Biochem J 2013; 449: 11-23.
[6] Kosnopfel C, Sinnberg T and Schittek B. Y-box binding protein 1-a prognostic marker and target in tumour therapy. Eur J Cell Biol 2014; 93: 61-70.
[7] Maurya PK, Mishra A, Yadav BS, Singh S, Kumar P, Chaudhary A, Srivastava S, Murugesan SN and Mani A. Role of Y box protein-1 in cancer: as potential biomarker and novel therapeutic target. J Cancer 2017; 8: 1900-1907.
[8] Johnson TG, Schelch K, Mehta S, Burgess A and Reid G. Why be one protein when you can affect many? The multiple roles of YB-1 in lung cancer and mesothelioma. Front Cell Dev Biol 2019; 7: 221.
[9] Sangermano F, Delicato A and Calabro V. Y box binding protein 1 (YB-1) oncoprotein at the hub of DNA proliferation, damage and cancer progression. Biochimie 2020; 179: 205-216.
[10] Alkrekshi A, Wang W, Rana PS, Markovic V and Sossey-Alaoui K. A comprehensive review of the functions of YB-1 in cancer stemness, metastasis and drug resistance. Cell Signal 2021; 85: 110073.
[11] Lettau K, Khozooei S, Kosnopfel C, Zips D, Schittek B and Toulany M. Targeting the Y-box binding protein-1 axis to overcome radiochemotherapy resistance in solid tumors. Int J Radiat Oncol Biol Phys 2021; 111: 1072-1087.
[12] Yin Q, Zheng M, Luo Q, Jiang D, Zhang H and Chen C. YB-1 as an oncoprotein: functions, regulation, post-translational modifications, and targeted therapy. Cells 2022; 11: 1217.
[13] Prabhu L, Hartley AV, Martin M, Warsame F, Sun E and Lu T. Role of post-translational modification of the Y box binding protein 1 in human cancers. Genes Dis 2015; 2: 240-246.
[14] Zhang J, Fan JS, Li S, Yang Y, Sun P, Zhu Q, Wang J, Jiang B, Yang D and Liu M. Structural basis of DNA binding to human YB-1 cold shock domain regulated by phosphorylation. Nucleic Acids Res 2020; 48: 9361-9371.
[15] Shah A, Lindquist JA, Rosendahl L, Schmitz I and Mertens PR. Novel insights into YB-1 signaling and cell death decisions. Cancers (Basel) 2021; 13: 3306.
[16] Pagano C, di Martino O, Ruggiero G, Maria Guarino A, Mueller N, Siauciunaite R, Reischl M, Simon Foulkes N, Vallone D and Calabro V. The tumor-associated YB-1 protein: new player in the circadian control of cell proliferation. Oncotarget 2017; 8: 6193-6205.
[17] Seeler JS and Dejean A. SUMO and the robustness of cancer. Nat Rev Cancer 2017; 17: 184-197.
[18] Zhao X. SUMO-mediated regulation of nuclear functions and signaling processes. Mol Cell 2018; 71: 409-418.
[19] Chang HM and Yeh ETH. SUMO: from bench to bedside. Physiol Rev 2020; 100: 1599-1619.
[20] Yau TY, Molina O and Courey AJ. SUMOylation in development and neurodegeneration. Development 2020; 147: dev175703.
[21] Xie M, Yu J, Ge S, Huang J and Fan X. SUMOylation homeostasis in tumorigenesis. Cancer Lett 2020; 469: 301-309.
[22] Flotho A and Melchior F. Sumoylation: a regulatory protein modification in health and disease. Annu Rev Biochem 2013; 82: 357-385.
[23] Han ZJ, Feng YH, Gu BH, Li YM and Chen H. The post-translational modification, SUMOylation, and cancer (Review). Int J Oncol 2018; 52: 1081-1094.
[24] Zeng M, Liu W, Hu Y and Fu N. Sumoylation in liver disease. Clin Chim Acta 2020; 510: 347-353.
[25] Johnson ES. Protein modification by SUMO. Annu Rev Biochem 2004; 73: 355-382.
[26] Lumpkin RJ, Gu H, Zhu Y, Leonard M, Ahmad AS, Clauser KR, Meyer JG, Bennett EJ and Komives EA. Site-specific identification and quantitation of endogenous SUMO modifications under native conditions. Nat Commun 2017; 8: 1171.
[27] Hendriks IA, Lyon D, Su D, Skotte NH, Daniel JA, Jensen LJ and Nielsen ML. Site-specific characterization of endogenous SUMOylation across species and organs. Nat Commun 2018; 9: 2456.
[28] Lascorz J, Codina-Fabra J, Reverter D and Torres-Rosell J. SUMO-SIM interactions: from structure to biological functions. Semin Cell Dev Biol 2022; 132: 193-202.
[29] Yau TY, Sander W, Eidson C and Courey AJ. SUMO interacting motifs: structure and function. Cells 2021; 10: 2825.
[30] Lin DY, Huang YS, Jeng JC, Kuo HY, Chang CC, Chao TT, Ho CC, Chen YC, Lin TP, Fang HI, Hung CC, Suen CS, Hwang MJ, Chang KS, Maul GG and Shih HM. Role of SUMO-interacting motif in Daxx SUMO modification, subnuclear localization, and repression of sumoylated transcription factors. Mol Cell 2006; 24: 341-354.
[31] Meulmeester E, Kunze M, Hsiao HH, Urlaub H and Melchior F. Mechanism and consequences for paralog-specific sumoylation of ubiquitin-specific protease 25. Mol Cell 2008; 30: 610-619.
[32] Li GM. Mechanisms and functions of DNA mismatch repair. Cell Res 2008; 18: 85-98.

[33] Kunkel TA and Erie DA. Eukaryotic mismatch repair in relation to DNA replication. Annu Rev Genet 2015; 49: 291-313.
[34] Liu D, Keijzers G and Rasmussen LJ. DNA mismatch repair and its many roles in eukaryotic cells. Mutat Res 2017; 773: 174-187.
[35] Huang Y and Li GM. DNA mismatch repair in the context of chromatin. Cell Biosci 2020; 10: 10.
[36] Li SKH and Martin A. Mismatch repair and colon cancer: mechanisms and therapies explored. Trends Mol Med 2016; 22: 274-289.
[37] Baretti M and Le DT. DNA mismatch repair in cancer. Pharmacol Ther 2018; 189: 45-62.
[38] Germano G, Amirouchene-Angelozzi N, Rospo G and Bardelli A. The clinical impact of the genomic landscape of mismatch repair-deficient cancers. Cancer Discov 2018; 8: 1518-1528.
[39] Zhao P, Li L, Jiang X and Li Q. Mismatch repair deficiency/microsatellite instability-high as a predictor for anti-PD-1/PD-L1 immunotherapy efficacy. J Hematol Oncol 2019; 12: 54.
[40] He Y, Zhang L, Zhou R, Wang Y and Chen H. The role of DNA mismatch repair in immunotherapy of human cancer. Int J Biol Sci 2022; 18: 2821-2832.
[41] Kunkel TA and Erie DA. DNA mismatch repair. Annu Rev Biochem 2005; 74: 681-710.
[42] Jiricny J. Postreplicative mismatch repair. Cold Spring Harb Perspect Biol 2013; 5: a012633.
[43] Kolodner RD. A personal historical view of DNA mismatch repair with an emphasis on eukaryotic DNA mismatch repair. DNA Repair (Amst) 2016; 38: 3-13.
[44] Modrich P. Mechanisms in E. coli and human mismatch repair (Nobel Lecture). Angew Chem Int Ed Engl 2016; 55: 8490-8501.
[45] Huang Y and Li GM. DNA mismatch repair preferentially safeguards actively transcribed genes. DNA Repair (Amst) 2018; 71: 82-86.
[46] Wessbecher IM and Brieger A. Phosphorylation meets DNA mismatch repair. DNA Repair (Amst) 2018; 72: 107-114.
[47] Masih PJ, Kunnev D and Melendy T. Mismatch repair proteins are recruited to replicating DNA through interaction with proliferating cell nuclear antigen (PCNA). Nucleic Acids Res 2008; 36: 67-75.
[48] Chang YW, Mai RT, Fang WH, Lin CC, Chiu CC and Wu Lee YH. YB-1 disrupts mismatch repair complex formation, interferes with MutSalpha recruitment on mismatch and inhibits mismatch repair through interacting with PCNA. Oncogene 2014; 33: 5065-5077.
[49] Fu D, Calvo JA and Samson LD. Balancing repair and tolerance of DNA damage caused by alkylating agents. Nat Rev Cancer 2012; 12: 104-120.
[50] Li Z, Pearlman AH and Hsieh P. DNA mismatch repair and the DNA damage response. DNA Repair (Amst) 2016; 38: 94-101.
[51] Gupta D and Heinen CD. The mismatch repair-dependent DNA damage response: mechanisms and implications. DNA Repair (Amst) 2019; 78: 60-69.
[52] Roos WP and Kaina B. DNA damage-induced cell death: from specific DNA lesions to the DNA damage response and apoptosis. Cancer Lett 2013; 332: 237-248.
[53] Ijsselsteijn R, Jansen JG and de Wind N. DNA mismatch repair-dependent DNA damage responses and cancer. DNA Repair (Amst) 2020; 93: 102923.
[54] Calderon-Montano JM, Burgos-Moron E, Orta ML and Lopez-Lazaro M. Effect of DNA repair deficiencies on the cytotoxicity of drugs used in cancer therapy - a review. Curr Med Chem 2014; 21: 3419-3454.
[55] Wang WT, Tsai TY, Chao CH, Lai BY and Wu Lee YH. Y-box binding protein 1 stabilizes hepatitis C virus NS5A via phosphorylation-mediated interaction with NS5A to regulate viral propagation. J Virol 2015; 89: 11584-11602.
[56] Mai RT, Yeh TS, Kao CF, Sun SK, Huang HH and Wu Lee YH. Hepatitis C virus core protein recruits nucleolar phosphoprotein B23 and coactivator p300 to relieve the repression effect of transcriptional factor YY1 on B23 gene expression. Oncogene 2006; 25: 448-462.
[57] Chuang SE, Doong SL, Lin MT and Cheng AL. Tax of the human T-lymphotropic virus type I transactivates promoter of the MDR-1 gene. Biochem Biophys Res Commun 1997; 238: 482-486.
[58] Shih CM, Lo SJ, Miyamura T, Chen SY and Lee YH. Suppression of hepatitis B virus expression and replication by hepatitis C virus core protein in HuH-7 cells. J Virol 1993; 67: 5823-5832.
[59] Deng Z, Wan M and Sui G. PIASy-mediated sumoylation of Yin Yang 1 depends on their interaction but not the RING finger. Mol Cell Biol 2007; 27: 3780-3792.
[60] You LR, Chen CM, Yeh TS, Tsai TY, Mai RT, Lin CH and Lee YH. Hepatitis C virus core protein interacts with cellular putative RNA helicase. J Virol 1999; 73: 2841-2853.
[61] Tatham MH, Jaffray E, Vaughan OA, Desterro JM, Botting CH, Naismith JH and Hay RT. Polymeric chains of SUMO-2 and SUMO-3 are conjugated to protein substrates by SAE1/SAE2 and Ubc9. J Biol Chem 2001; 276: 35368-35374.
[62] Geiss-Friedlander R and Melchior F. Concepts in sumoylation: a decade on. Nat Rev Mol Cell Biol 2007; 8: 947-956.

[63] Zhao J. Sumoylation regulates diverse biological processes. Cell Mol Life Sci 2007; 64: 3017-3033.
[64] Blanco G and Mercer RW. Isozymes of the Na-K-ATPase: heterogeneity in structure, diversity in function. Am J Physiol 1998; 275: F633-650.
[65] Lingrel JB, Croyle ML, Woo AL and Arguello JM. Ligand binding sites of Na,K-ATPase. Acta Physiol Scand Suppl 1998; 643: 69-77.
[66] Stojic L, Cejka P and Jiricny J. High doses of SN1 type methylating agents activate DNA damage signaling cascades that are largely independent of mismatch repair. Cell Cycle 2005; 4: 473-477.
[67] Chang CC, Naik MT, Huang YS, Jeng JC, Liao PH, Kuo HY, Ho CC, Hsieh YL, Lin CH, Huang NJ, Naik NM, Kung CC, Lin SY, Chen RH, Chang KS, Huang TH and Shih HM. Structural and functional roles of Daxx SIM phosphorylation in SUMO paralog-selective binding and apoptosis modulation. Mol Cell 2011; 42: 62-74.
[68] Hardeland U, Steinacher R, Jiricny J and Schar P. Modification of the human thymine-DNA glycosylase by ubiquitin-like proteins facilitates enzymatic turnover. EMBO J 2002; 21: 1456-1464.
[69] Baba D, Maita N, Jee JG, Uchimura Y, Saitoh H, Sugasawa K, Hanaoka F, Tochio H, Hiroaki H and Shirakawa M. Crystal structure of thymine DNA glycosylase conjugated to SUMO-1. Nature 2005; 435: 979-982.
[70] Takahashi H, Hatakeyama S, Saitoh H and Nakayama KI. Noncovalent SUMO-1 binding activity of thymine DNA glycosylase (TDG) is required for its SUMO-1 modification and colocalization with the promyelocytic leukemia protein. J Biol Chem 2005; 280: 5611-5621.

Table S1. Primers used for site-directed mutagenesis to generate YB-1 mutant-expressing constructs

Primer	Sequence*
YB-1/K26R-F	GCCGCCGACACCAGGCCCGGCACTAC
YB-1/K26R-R	GTAGTGCCGGGCCTGGTGTCGGCGGC
YB-1/K52.53R-F	CCTGCCGGCGGGGACAGGAGGGTCATCGCAACGAAGG
YB-1/K52.53R-R	CCTTCGTTGCGATGACCCTCCTGTCCCCGCCGGCAGG
YB-1/K58R-F	CAAGAAGGTCATCGCAACGAGGGTTTTGGGAACAGTAAAATGG
YB-1/K58R-R	CCATTTTACTGTTCCCAAAACCCTCGTTGCGATGACCTTCTTG
YB-1/K64R-F	CGAAGGTTTTGGGAACAGTAAGATGGTTCAATGTAAGGAACGG
YB-1/K64R-R	CCGTTCCTTACATTGAACCATCTTACTGTTCCCAAAACCTTCG
YB-1/K81R-F	CATCAACAGGCCTGACACCAGGGAAGATGTATTTGTACACC
YB-1/K81R-R	GGTGTACAAATACATCTTCCCTGGTGTCATTCCTGTTGATG
YB-1/K92.93R-F	GTACACCAGACTGCCATAAGGAGGAATAACCCCAGGAAGTACC
YB-1/K92.93R-R	GGTACTTCCTGGGGTTATTCCTCCTTATGGCAGTCTGGTGTAC
YB-1/K98R-F	GAATAACCCCAGGAGGTACCTTCGCAGTGTAGG
YB-1/K98R-R	CCTACACTGCGAAGGTACCTCCTGGGGTTATTC
YB-1/K118R-F	GTTGTTGAAGGAGAAAGGGGTGCGGAGGCAGC
YB-1/K118R-R	GCTGCCTCCGCACCCCTTTCTCCTTCAACAAC
YB-1/K137R-F	GGTGGTGTTCCAGTTCAAGGCAGTAGATATGCAGCAGAC
YB-1/K137R-R	GTCTGCTGCATATCTACTGCCTTGAACTGGAACACCACC
YB-1/K170R-F	GAATAGTGAGAGTGGGGAAAGGAACGAGGGATCGGAGAGTGC
YB-1/K170R-R	GCACTCTCCGATCCCTCGTTCCTTTCCCCACTCTCACTATTC
YB-1/K264R-F	GGACGGCAATGAAGAAGATAGAGAAAATCAAGGAGATGAG
YB-1/K264R-R	CTCATCTCCTTGATTTTCTCTATCTTCTTCATTGCCGTCC
YB-1/K296R-F	GACGCCCAGAAAACCCTAGACCACAAGATGGC
YB-1/K296R-R	GCCATCTTGTGGTCTAGGGTTTTCTGGGCGTC
YB-1/K301.304R-F	CCACAAGATGGCAGAGAGACAAGAGCAGCCGATCCACC
YB-1/K301.304R-R	GGTGGATCGGCTGCTCTTGTCTCTCTGCCATCTTGTGG
YB-1/V113.114A-F	GGAGAGACTGTGGAGTTTGATGCTGCTGAAGGAGAAAAGGG
YB-1/V113.114A-R	CCCTTTTCTCCTTCAGCAGCATCAAACTCCACAGTCTCTCC
YB-1/V131.133A-F	GGTCCTGGTGGTGCTCCAGCTCAAGGCAGTAAATATGC
YB-1/V131.133A-R	GCATATTTACTGCCTTGAGCTGGAGCACCACCAGGACC

*The underlined letters in the sequences of the mutagenic primers indicate the nucleotide substitutions that generated the desired mutations.

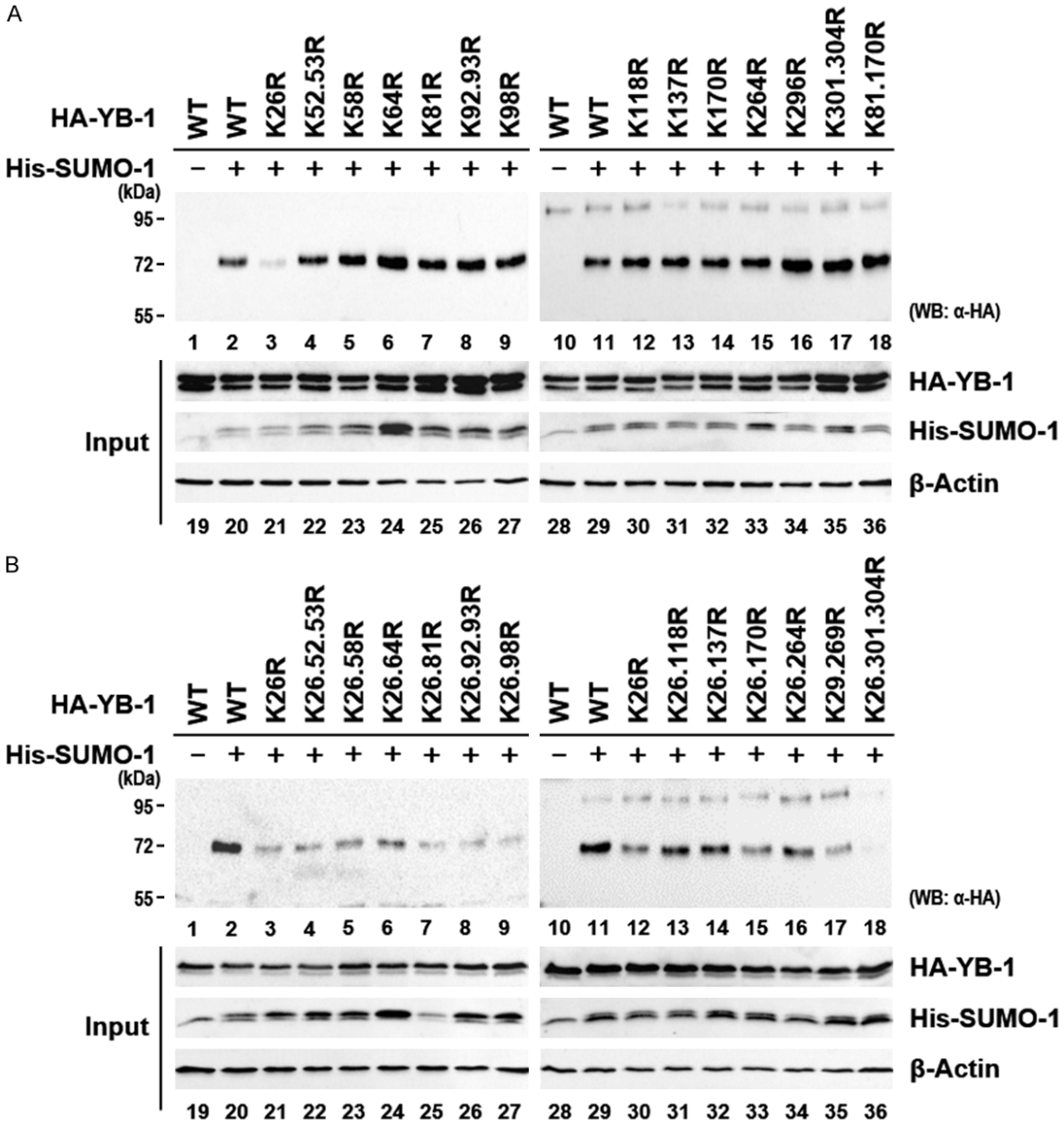

Figure S1. *In vivo* sumoylation assay with various lysine-to-arginine HA-YB-1 mutants. (A) Plasmids expressing wild-type HA-YB-1 or its mutants, His-SUMO-1, and Flag-Ubc9 were co-transfected into HEK-293T cells as indicated at the top of each panel. Cells were harvested 48 h post transfection and subjected to an *in vivo* sumoylation assay in the presence of N-ethylmaleimide. Proteins bound to Ni-NTA agarose were analyzed by western blotting with an anti-HA tag antibody (lanes 1-18). Cellular expression of individual construct was confirmed by immunoblotting using the appropriate antibodies (lanes 19-36). β-Actin was used as a loading control. (B) An *in vivo* sumoylation assay similar to that described in (A) was performed, except that plasmids expressing different HA-YB-1 mutants were used as indicated (lanes 1-18). To confirm the cellular expression of individual construct in cells, lysates were also subjected to immunoblotting using the appropriate antibodies (lanes 19-36). β-Actin was used as a loading control.

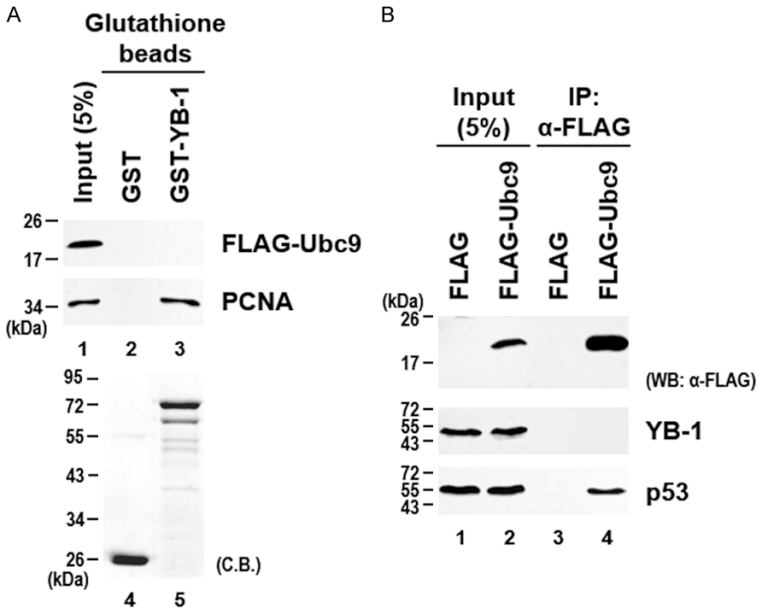

Figure S2. YB-1 does not interact with Ubc9. (A) The plasmid expressing FLAG-Ubc9 was transfected into HEK293T cells. Whole-cell lysates were prepared 48 h post transfection and were subjected to an *in vitro* binding assay with glutathione-Sepharose 4B beads-bound GST or GST-YB-1. Whole-cell lysates (25 μg, lane 1) and proteins bound to the beads (lanes 2-3) were analyzed by western blotting using antibodies against the FLAG tag or PCNA. Purified GST and GST-YB-1 were analyzed by SDS-PAGE and stained with Coomassie brilliant blue (C.B., lanes 4-5). PCNA served as a positive control for YB-1-interacting protein, as demonstrated in our previous study [1]. (B) The plasmid expressing FLAG-Ubc9 or the corresponding empty vector (FLAG) was transfected into HEK293T cells. Whole-cell lysates were prepared 48 h post transfection and were subjected to a co-immunoprecipitation assay with anti-FLAG M2 magnetic beads. Whole-cell lysates (25 μg each, lanes 1-2) and proteins bound to the beads (lanes 3-4) were analyzed by western blotting using antibodies against the FLAG tag (#2368, Cell Signaling Technology), YB-1, and p53 (#9282, Cell Signaling Technology). p53 served as a positive control for Ubc9-interacting protein, as reported in a previous study [2].

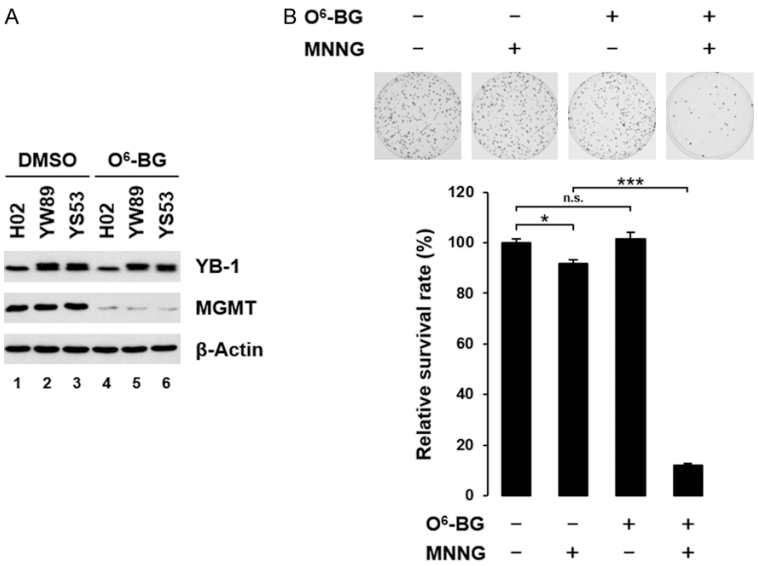

Figure S3. The MGMT inhibitor O^6-benzylguanine sensitizes HeLa cells to MNNG-induced cytotoxicity. (A) Vector control cells (H02) as well as cells with stable overexpression of HA-YB-1 (YW89) or HA-YB-1/K26R (YS53) were treated with 25 μM O^6-benzylguanine (O^6-BG) for 24 h, and cell lysates were then analyzed by western blotting with anti-YB-1, anti-MGMT, and anti-β-actin antibodies. β-Actin was used as a loading control. (B) Prior to MNNG treatment, HeLa cells were cultured in complete medium with or without 25 μM O^6-BG. After treatment with 0.05 μM MNNG for 3 h, the cells were reseeded at a density of ~400 cells per 10-cm dish and incubated for 14 days. Colonies were fixed with 1:1 acetone:ethanol and stained with 0.05% crystal violet. Surviving colonies were counted, and the numbers of colonies were normalized to that the number of colonies formed by untreated cells. The results were derived from three independent experiments, and the error bars indicate ±1 s.d. of the mean. Statistical analyses were carried out using one-way ANOVA and Tukey's post hoc test (n.s., not significant, $P > 0.05$; *, $P < 0.05$; ***, $P < 0.001$).

References

[1] Chang YW, Mai RT, Fang WH, Lin CC, Chiu CC and Wu Lee YH. YB-1 disrupts mismatch repair complex formation, interferes with MutSalpha recruitment on mismatch and inhibits mismatch repair through interacting with PCNA. Oncogene 2014; 33: 5065-5077.

[2] Lin JY, Ohshima T and Shimotohno K. Association of Ubc9, an E2 ligase for SUMO conjugation, with p53 is regulated by phosphorylation of p53. FEBS Lett 2004; 573: 15-18.